



Dalton
Transactions

**Imidazolyl-Phenyl (IMP) Anions: A Modular Structure for
Tuning Solubility and Coordinating Ability**

| | |
|-------------------------------|---|
| Journal: | <i>Dalton Transactions</i> |
| Manuscript ID | DT-ART-08-2019-003511 |
| Article Type: | Paper |
| Date Submitted by the Author: | 29-Aug-2019 |
| Complete List of Authors: | Wozniak, Derek; Temple University Hicks, Andrew; Temple University Sabbers, William; Temple University Dobereiner, Graham; Temple University |
| | |

SCHOLARONE™
Manuscripts

PAPER

Imidazolyl-Phenyl (IMP) Anions: A Modular Structure for Tuning Solubility and Coordinating Ability†

Derek I. Wozniak, Andrew J. Hicks, William A. Sabbers, and Graham E. Dobereiner*

Received 00th January 20xx,
Accepted 00th January 20xx

DOI: 10.1039/x0xx00000x

The effect of counteranion upon a cation's solution-phase reactivity depends on a subtle interplay of weak interactions. Although these effects are widely appreciated in synthesis and catalysis, probing and controlling anion-cation interactions remains a significant challenge. Here we report the synthesis, characterisation and reactivity of the IMP anions, a family of anions with a coordinating ability that can be tuned for a given application. The anions are robust, compatible with both strongly basic and acidic media, suitable for isolation of unstable organometallic species, and effective as counteranions for homogeneous catalysis. IMP anions are prepared in two steps: deprotonation of substituted 2-phenylimidazoles with NaH, followed by addition of 2 equiv. $B(C_6F_5)_3$. The anions prepared feature a range of functionality, including nitro, ester, amide, amine and alcohol groups. Based on the spectroscopic properties of $[Pd(IPr)(C(O)C_9H_6N)] [IMP-R]$, the coordinating ability of $[IMP-R]^-$ ranges between BF_4^- and $BArF_4^-$, depending on the polarity of the R group. Gold complexes of type $[L-Au-L'] [IMP-R]$ have been isolated and characterised, resulting in the first X-ray structure of a $(\eta^2$ -diphenylacetylene)Au complex. $[(tBuXPhos)Au(MeCN)] [IMP-R]$ catalyses [2+2] cyclisation of alkenes and alkynes, as well as the hydroalkoxylation of alkynes. Unlike SbF_6^- and $BArF_4^-$, the $[IMP-H]^-$ and $[IMP-CF_3]^-$ salts are sufficiently soluble to efficiently promote cyclisations in toluene with $[(tBuXPhos)Au(MeCN)]^+$.

Introduction

Weakly-coordinating anions (WCAs; Fig. 1)¹⁻⁴ enable isolation of highly electrophilic species⁵⁻⁷ and play essential roles in homogeneous catalysis.⁸⁻¹⁰ Anions compete with solvent, ancillary ligands, substrate, and potentially product, for inner-sphere binding to a cationic metal centre's coordination sites. The most weakly-binding anions therefore permit cations to interact with substrate with minimal competition from anion.¹¹ Highly lipophilic anions also solubilise catalysts in weakly-binding solvents, permitting catalysis in media that minimizes competitive coordination of solvent to binding sites.^{11, 12} Weak anion coordination is often beneficial for catalytic rates, although coordination can also protect catalytic intermediates against deactivation.^{13, 14} These inner-sphere phenomena are discrete from ion-pair aggregation or outer-sphere interactions with substrate-coordinated complexes, which can further attenuate the behaviour of catalytic intermediates and influence barriers to product. The complex nature of the equilibria that depend on inner-sphere anion binding, combined with the weak and unpredictable nature of outer-sphere interactions, makes it very difficult to determine an ideal anion for a given organometallic application without extensive empirical exploration.

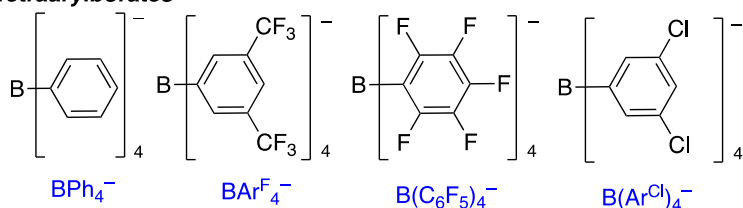
Although "superweak" anions, such as the charge-diffuse halogenated tetraarylborate $BArF_4^-$,¹⁵⁻¹⁸ have been widely adopted in catalysis, some catalytic reactions actually demonstrate superior activity and selectivity in the presence of more tightly-coordinating anions.¹⁹⁻²⁵ In gold(I) catalysis, basic counteranions are thought to participate in cooperative reactions with cationic intermediates.^{19-21, 24, 26-31} Toste and coworkers^{32, 33} have pioneered a chiral counteranion strategy for Au(I) catalysis, where chiral anions associated through ion-pairing and/or hydrogen bonding engage substrate during a stereoselectivity-determining step. Zuccaccia, Belanzoni and coworkers¹⁹⁻²¹ and Zhdanko and Maier²⁴ have explored anion effects in Au-catalysed alkyne hydroalkoxylation, finding OTs^- and OTf^- promote nucleophilic attack by hydrogen bonding with the alcohol nucleophile; more weakly-coordinating anions (SbF_6^-) are inferior hydrogen bond acceptors and are far less effective. At the other extreme, more strongly coordinating and basic anions (OAc^- , TFA^-) bind too well to Au for facile substrate binding, and can further deactivate catalyst by formation of Au-OR. Here a balance in basicity is key to achieving the highest catalytic rates.

Because anions can play various roles in catalysis,³⁴⁻³⁶ extensive screening may be needed before an effective counteranion and solvent is identified. Stability of anion and compatibility with cation are other important considerations.³⁷ Just like ligands, various physical properties of anions – solubility, basicity, hydrogen bonding/proton affinity, metal affinity – can influence reaction outcomes, but unlike the myriad variants of highly modular phosphorus and carbene

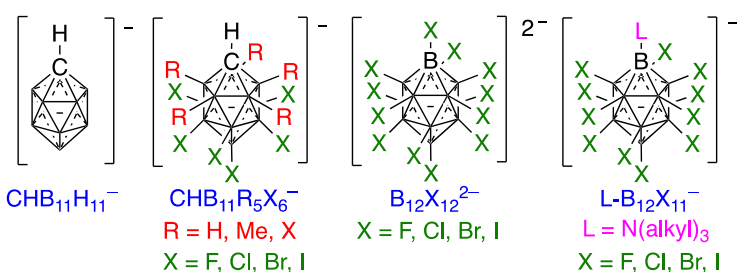
Department of Chemistry, Temple University, Philadelphia, PA 19122, United States. E-mail: dob@temple.edu

† Electronic supplementary information (ESI) available: NMR and IR spectra. CCDC 1919818-1919840. For ESI and crystallographic data in CIF or other electronic format see DOI: 10.1039/x0xx00000x

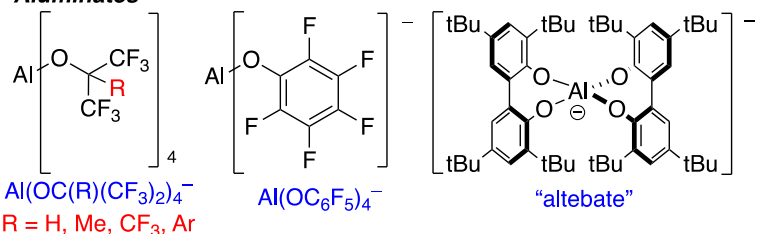
Tetraarylborates



Carboranes and dodecaboranes



Aluminates



Bridged WCAs

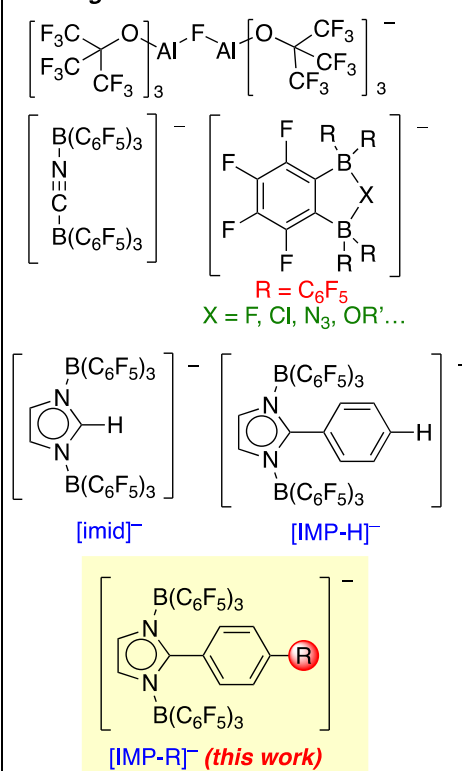


Fig 1 Selected examples of modular weakly-coordinating anionic scaffolds.

ligand classes employed by organometallics chemists, most catalytic explorations rely on a small collection of "traditional" anions (e.g., ClO_4^- , BF_4^- , and PF_6^-). These anions are, in general, less charge-diffuse and more coordinating^{38, 39} than modern WCAs such as borates, aluminates, and halogenated or alkylated carboranes;^{1-3, 40-43} they are also, in general, more structurally heterogeneous than modern WCAs and vary dramatically in physical properties from one another.

A systematic approach to tuning anion coordinating ability would be useful in empirical optimisation of catalytic conditions, especially in cases where anion functionality facilitates a key step. More broadly, controlling the hydrophobicity of counteranions permits "fine-tuning" in the rational design for synthetic routes, including construction of ionic liquids and soft (polymer) materials.⁴⁴ Another potential use is in exploring the structure/activity relationships within a mechanistic study. Computational approaches to considering ion-pairing effects have led to important insights,⁴⁵ and examination of solid-phase data provides a comparison of weakly-coordinating character.⁴⁶ However, pinpointing the role of anions in solution-phase reactions remains challenging because weak anion/cation solution interactions are difficult to measure. Several NMR techniques are available for quantification if key resonances can be observed *in situ*.^{11, 47-49} Granular adjustments to anion coordinating ability could reveal potential roles of counteranion during catalysis, offering a broader understanding of underlying mechanisms. Employing Zwitterionic complexes, featuring ligands that combine robust

metal-ligand connectivity with a pendant weakly-coordinating anionic element,⁵⁰⁻⁵⁶ can yield valuable insights into counteranion effects.

Surprisingly, tuneable weakly-coordinating anions that engage metals with weak, transient dative bonds have not been used widely to study and control anion effects in organometallic catalysis. Select modern WCA anion scaffolds that could be used for fine-tuning of anion effects are highlighted in Fig. 1. These scaffolds combine stability in acidic and basic media with expansive synthetic versatility. One class, the tetraarylborates, show variable coordinating ability depending on the extent of halogenation on the aromatic rings. The η^6 -arene coordination³ common for BPh_4^- can be reduced with partial fluorination (BARF_4^-); π -coordination of the perfluorinated arenes of $\text{B}(\text{C}_6\text{F}_5)_4^-$ has not yet been observed crystallographically.² Similarly, a wide variety of *closo*-carboranes and dodecaboranes with diverse coordinating ability and solubility properties can be formed via reaction at either the carbon vertex or boron vertices of $\text{CHB}_{11}\text{H}_{11}^-$.⁴³ Carboranes of type $[\text{CHB}_{11}\text{R}_5\text{X}_6]^-$ ($\text{R} = \text{H, Me, X}$; $\text{X} = \text{F, Cl, Br, I}$) have a balance of high thermal stability, good solubility⁵⁷ and tuneable coordinating ability⁵⁸ that has been useful for stabilizing extremely electrophilic species.⁵ More recent efforts exploring applications beyond the conventional WCA contexts showcase the synthetic breadth of carboranes.^{41, 42} Finally, aluminates can be modified through modifying the alkoxy, aryloxy or anilide substituents.⁵⁹ For example, While $[\text{Al}(\text{OC}(\text{CF}_3)_2)_4]^-$ is very weakly coordinating and

stable to protonolysis,⁶⁰ biphenolic aluminates such as “albeate”⁶¹ are highly lipophilic yet unstable in protic media.⁶²

The present work describes the synthesis and properties of a “bridged WCA”² platform. Prior examples of this class include Bochmann’s $[(F_5C_6)_3B-LB-B(C_6F_5)_3]^-$ ⁶³⁻⁶⁵ (LB = CN, NH₂, etc.), Ingo-Krossing’s $[(F_3C)_3CO)_3Al(\mu-F)Al(OC(CF_3)_3)_3]^-$,⁶⁶ and Piers’ chelating diborane^{67, 68} (Fig. 1). These anions are Lewis acid/base adducts where two large lipophilic Lewis acids are bound to a single monoanionic ligand, forming an even larger and more charge-diffuse structure.² The parent of our anion family,³⁴ the weakly-coordinating phenylimidazole-based anion ([IMP-H]⁻, Fig. 1) is itself a derivative of the superweak [imid]⁻ bridged WCA prepared by LaPointe, Klosin, Babb and co-workers^{69, 70} and part of a broader class of borane-adduct bridged WCAs.^{63-65, 71-73}

The IMP anion family we report is simple to synthesise, air- and moisture-stable, and features an array of installed functionalities. [IMP-R]⁻ anions have been paired with $[Pd(IPr)(C(O)C_9H_6N)]^+$ (**1**) to assess donor abilities³⁴ via NMR, IR, DFT, and percent buried volume. Preliminary examination of counteranion effects have been explored in Au-catalysed intermolecular [2+2] cyclisation of phenylacetylene with α -methyl styrene as well as the Au-catalysed alkoxylation of 3-hexyne with two different nucleophiles. We find that the choice of installed anion functionality affects the coordinating ability of the IMP anions as well as their solubility, and therefore serves as a means to control the structure and reactivity of organometallic cations.

Results

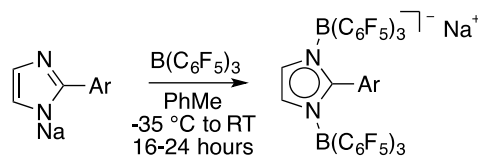
Synthesis and Characterisation of Na[IMP-R] Salts.

Deprotonation of substituted 2-phenylimidazoles or 2-phenylbenzimidazole with NaH followed by addition of $B(C_6F_5)_3$ at $-35\text{ }^\circ\text{C}$ yields the sodium salts of [IMP-R]⁻ (Table 1). Benzimidazole-based [BIMP]⁻ was prepared similarly (Fig. 2). In our hands Li imidazolates were incompatible with $B(C_6F_5)_3$ and formed other products, but once prepared, [IMP-R]⁻ are stable to Li⁺ including in strongly basic and reducing conditions. For example, lithium aluminium hydride reduction of Na[IMP-CO₂Me] and Na[IMP-DMA] affords the benzyl alcohol- and benzyl amine-substituted anions [IMP-CH₂OH] and [IMP-CH₂NMe₂] (Fig. 2).

The salts are indefinitely air- and moisture-stable, and in our hands less hygroscopic than $NaBAR^f_4$. Recrystallisation of anions from dichloromethane/tetrahydrofuran/pentane results in $Na(THF)_x[IMP-R]$. Like the parent [imid]⁻ anion (Fig. 1),⁶⁹ the bond distances of the anion’s phenylimidazolato core are essentially the same as those of the parent imidazoles. For example, bond parameters of 4-(1H-imidazol-2-yl)-N,N-dimethylbenzamide are nearly identical to Na[IMP-DMA]; 2-(3,5-bis(trifluoromethyl)phenyl)-1H-imidazole and Na[IMP-(CF₃)₂] also have similar bond lengths and angles (see structure reports for each in the ESI). In the obtained structures of Na[IMP-CO₂Me] (Fig. 3), Na[IMP-DMA], Na[IMP-DBA], and Na[IMP-pipA], Na⁺ coordinates to the anion C=O, with Na–O bonds ranging 2.25 – 2.32 Å. Na[IMP-CH₂OH] and Na[IMP-

CH₂NMe₂] show Na⁺ coordinating to the heteroatomic (O, N) anion functionality; Na[IMP-CH₂OH] further shows a 2.659(7) Å O–H...O hydrogen bond between –CH₂OH and cocrystallised THF (Fig. 3). Na[BIMP] demonstrates Na⁺ coordination to mutually *ortho*-fluorines on one C₆F₅ ring, while [IMP-(CF₃)₂] exhibits no contacts with Na⁺. On the whole, X-ray analysis shows the negative charge of [IMP-R]⁻ to be highly diffuse, such that coordination of *para*-substituents to Na⁺ mimics the behaviour of neutral organic molecules.

Table 1 IMP anions prepared via reaction of sodium imidazolates and $B(C_6F_5)_3$ ^a



| Anion | -Ar | Yield |
|--|--|-------|
| [IMP-CF ₃] | 4-(trifluoromethyl)phenyl | 62% |
| [IMP-(CF ₃) ₂] | 3,5-bis(trifluoromethyl)phenyl | 74% |
| [IMP-NO ₂] | 4-nitrophenyl | 62% |
| [IMP-CO ₂ Me] | 4-(methoxycarbonyl)phenyl | 56% |
| [IMP-DMA] | 4-(dimethylcarbamoyl)phenyl | 41% |
| [IMP-DBA] | 4-(di- <i>n</i> -butylcarbamoyl)phenyl | 46% |
| [IMP-pipA] | 4-(piperidine-1-carbonyl)phenyl | 77% |

^a See electronic supplementary Information (ESI) for synthetic procedures.

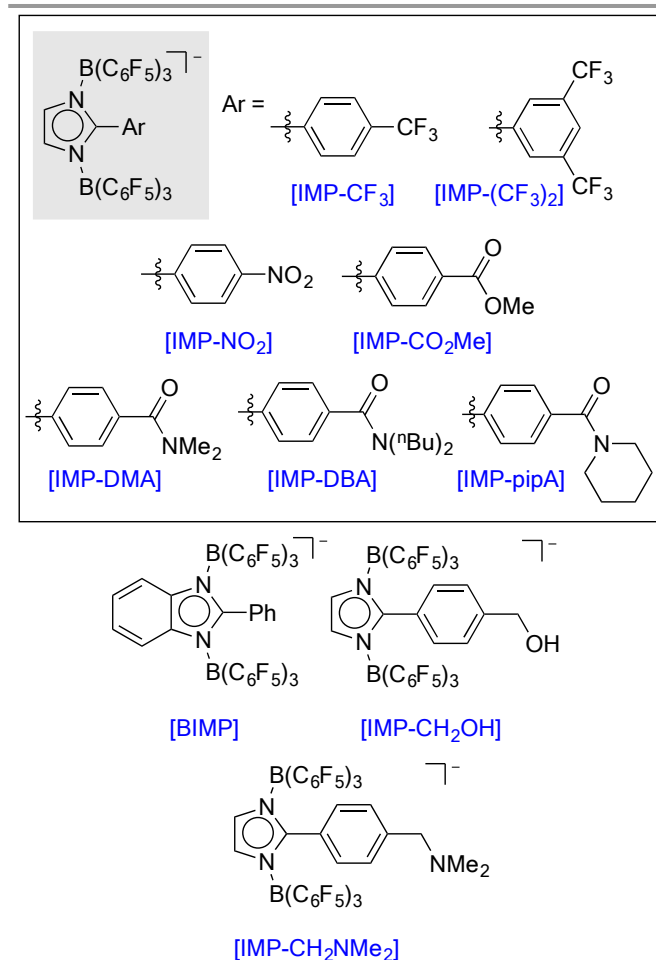


Fig. 2 Structures of anions prepared.

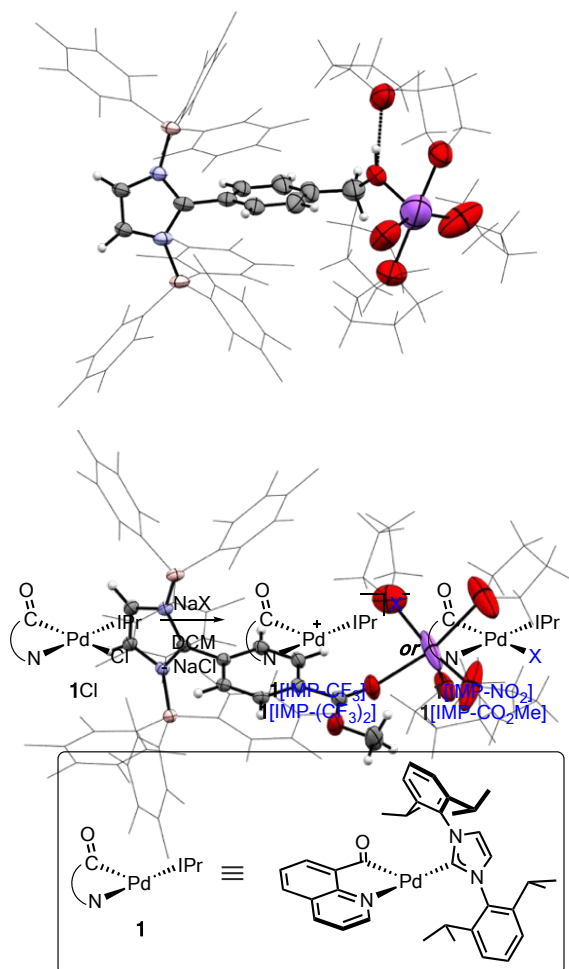


Fig. 3 Thermal ellipsoid plots of $\text{Na}[\text{IMP-CO}_2\text{Me}]$ (top) and $\text{Na}[\text{IMP-CH}_2\text{OH}]$ (bottom). Ellipsoids shown at 50% probability. THF and C_6F_5 rings shown as wireframe for clarity. $\text{O-H}\cdots\text{O}$ hydrogen bond drawn with dashed line.

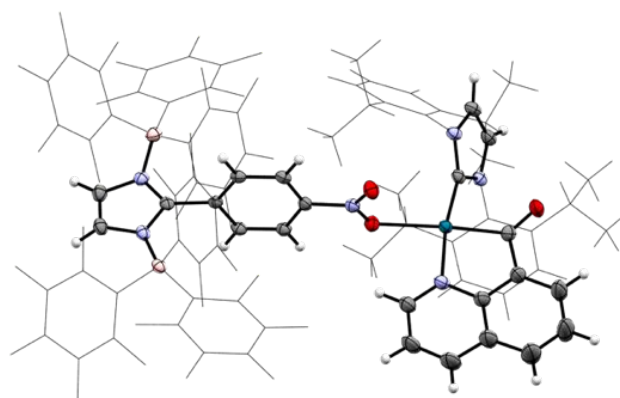
Assessment of [IMP-R] Coordinating Ability. Pairing of $[\text{IMP-R}]^-$ with the $[\text{Pd}(\text{IPr})(\text{C}(\text{O})\text{C}_9\text{H}_6\text{N})]$ cation (**1**) allowed us to use several metrics previously reported by our group³⁴ to assess qualitative differences in donor ability in both solid and solution states in the context of Pd chemistry. With more tightly-binding anions (e.g., BF_4^- , OTf^- , ClO_4^-), complexes of **1** crystallise with counteranion bound in the primary coordination sphere; if the anion is sufficiently weakly-coordinating (SbF_6^- , BARF_4^-), IPr isopropyl groups instead will form agostic interactions to occupy the vacant site (Scheme 1).

Scheme 1 Synthesis of $1[\text{IMP-R}]$ complexes.

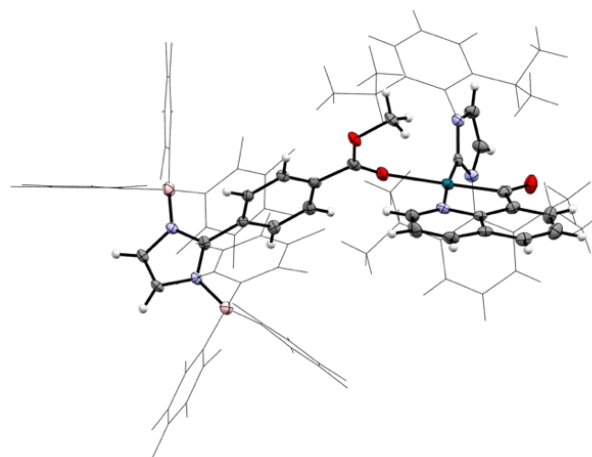
Addition of $\text{Na}[\text{IMP-R}]$ salts to a solution of **1Cl** followed by recrystallisation from dichloromethane/pentane or toluene/pentane resulted in X-ray quality crystals. Inner-sphere coordination was observed for $1[\text{IMP-NO}_2]$ and $1[\text{IMP-CO}_2\text{Me}]$ (Fig. 4). Both anions are bound to **1** via oxygen atoms, owing to the polarity of the nitro (N-O) and ester (C-O) bonds. $1[\text{IMP-CF}_3]$ and $1[\text{IMP-(CF}_3)_2]$ instead crystallise as outer-sphere ion pairs like the previously reported $1[\text{IMP-H}]$.³⁴

Fig. 4 Crystal structures of inner-sphere $1[\text{IMP-NO}_2]$ (top) and $1[\text{IMP-CO}_2\text{Me}]$ (bottom) complexes. C_6F_5 rings and diisopropylphenyl substituents shown in wireframe; solvent hidden for clarity. Ellipsoids shown at 50% probability.

The lipophilicity of the $\text{B}(\text{C}_6\text{F}_5)_3$ groups is apparently insufficient to impart dichloromethane (DCM) solubility to



complexes of the more basic $[\text{IMP-R}]^-$ variants. Upon adding **1Cl** to amide-containing $\text{Na}[\text{IMP-DMA}]$, $\text{Na}[\text{IMP-DBA}]$, or $\text{Na}[\text{IMP-pipA}]$ in DCM, bright yellow solids rapidly precipitated, likely *O*-bound inner-sphere complexes akin to $1[\text{IMP-CO}_2\text{Me}]$. The strength of amide binding may outcompete weakly-coordinating DCM and prevent dissolution. However, the yellow solids dissolve upon addition of more coordinating solvents. When recrystallised from DCM/pentane in the presence of



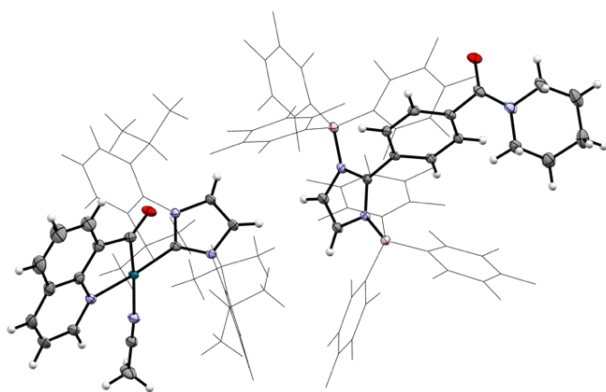


Fig. 5 Crystal structure of $[1(\text{MeCN})][\text{IMP-pipA}]$. Ellipsoids shown at 50% probability; C_6F_5 rings and diisopropylphenyl substituents shown in wireframe.

MeCN ion pairs can be cleanly isolated with MeCN bound in the fourth coordination site (for example, $[1(\text{MeCN})][\text{IMP-pipA}]$, Fig. 5). Solubility also complicated isolation of $1[\text{IMP-CH}_2\text{OH}]$ and $1[\text{IMP-CH}_2\text{NMe}_2]$, and in these cases the compounds could not be sufficiently purified for characterisation.

Beyond insights from solid-state structures, **1** is a useful probe of coordinating ability of anions in solution. When dissolved in DCM, anions weakly bound to **1** depart the primary coordination sphere, forming ion pairs. The IPr isopropyl methine chemical shift in ^1H NMR (CD_2Cl_2 , 298 K) correlates with the coordinating ability of the anion: the farther upfield the shift, the less interaction there is between cation and anion.³⁴ Based on this benchmark, soluble $1[\text{IMP-R}]$ compounds all fully dissociate in CD_2Cl_2 ; the cation/anion interactions of $1[\text{IMP-NO}_2]$ and $1[\text{IMP-CO}_2\text{Me}]$ observed in the solid state are apparently disrupted by DCM (Table 2). Since complexes $1[\text{IMP-R}]$ of the amide-functionalised anions are insoluble in CD_2Cl_2 they cannot be directly compared. Instead, $1[\text{IMP-DMA}]$ was dissolved in $\text{DMSO-}d_6$ and compared to $1[\text{BAR}_4^{\text{F}}]$. Although DMSO was expected to coordinate in both cases to form identical Pd environments, chemical shifts of Pd IPr and acylquinoline ligands differed substantially, suggesting $[\text{IMP-DMA}]^-$ retains some cation association – even in tightly coordinating DMSO.

Table 2 ^1H NMR Methine Chemical Shifts, Pd-Acyl C=O Frequencies, and $\%V_{\text{bur}}$ of complexes of **1**

| Anion | δ (ppm) | $\nu_{\text{C=O}}$, ATR-IR ^a | $\nu_{\text{C=O}}$, DCM ^a | $\%V_{\text{bur}}$ |
|---|----------------|---|--|--------------------|
| BAR_4^{F} ³⁴ | 2.75 | 1776 | 1760 | - |
| IMP-CF_3 | 2.74 | 1770 | 1761 | - |
| IMP-H ³⁴ | 2.75 | 1757 | 1760 | - |
| PF_6 ³⁴ | 2.75 | 1759 | 1760 | - |
| $\text{IMP-(CF}_3)_2$ | 2.75 | 1755 | 1761 | - |
| IMP-NO_2 | 2.76 | 1737 | 1760 | 16.9 |
| $\text{IMP-CO}_2\text{Me}$ | 2.76 | 1729 | 1761 | 18.7 |
| IMP-DMA | - ^b | 1695 | - ^b | - |
| IMP-pipA | - ^b | 1695 | - ^b | - |
| BF_4 ³⁴ | 2.89 | 1689 | 1760 | 14.2 |
| ClO_4 ³⁴ | 3.12 | 1684 | 1695 | 17.3 |

^a All frequencies in cm^{-1} . ^b Complexes are insoluble in DCM.

Solution-state IR spectroscopy also offers valuable information about the coordination environment of the Pd centre; the Pd-acyl C=O stretch shifts to lower energy when a donor is bound to the coordination site *trans* to the acyl.³⁴ Complexes of **1** exhibited nearly identical C=O stretches in solution, consistent with weakly-associated ion pairs (Table 2). In contrast, solid-state IR suggests $[\text{IMP-R}]^-$ anions range in coordinating ability. At one extreme, $[\text{IMP-CF}_3]^-$ is nearly as weakly coordinating as BAR_4^{F} ; meanwhile the more tightly-coordinating anions $[\text{IMP-DMA}]^-$ and $[\text{IMP-pipA}]^-$ provide as nearly as much electron density as BF_4 . While larger in volume than all of the traditional anions in Fig. 1, IMP anions are not symmetrical, and their steric profile depends upon coordination mode. Percent buried volume ($\%V_{\text{bur}}$) calculations carried out on X-ray structures of $1[\text{IMP-NO}_2]$ and $1[\text{IMP-CO}_2\text{Me}]$ using the *SambVca2* program⁷⁴ indicate both $[\text{IMP-NO}_2]^-$ and $[\text{IMP-CO}_2\text{Me}]^-$ have a $\%V_{\text{bur}}$ below the previously-determined threshold for binding to **1** ($< \sim 20\%$).³⁴ The methyl ester group imparts slightly more steric demand than the nitro group. $[\text{IMP-NO}_2]^-$ $\%V_{\text{bur}}$ (16.9%) is actually smaller than ClO_4^- (17.3%) when bound to **1**. Based on these calculations, the sterically demanding $\text{B}(\text{C}_6\text{F}_5)_3$ groups appear to offer only modest steric demand around the imidazolyl phenyl substituent. Coordination in the solid-state is mostly dependent on the donating character of the *para*-phenyl group.

[IMP-R] anions in Au catalysis. To assess the stability and compatibility of $[\text{IMP-R}]^-$ in organometallic reactions, we prepared $[\text{AuL}_n][\text{IMP-R}]$ complexes and compared activity to catalysts featuring traditional anions. $[\text{tBuXPhosAu}(\text{MeCN})]^+$ (**2**) shows counteranion-dependent activity in the [2+2] cyclisation of α -methyl styrene and phenylacetylene; Echavarren and coworkers⁷⁵⁻⁷⁸ found **2** $[\text{BAR}_4^{\text{F}}]$ and **2** $[\text{SbF}_6]$ ^{77, 78} to provide higher yields than more-coordinating anions (BF_4^- , PF_6^- , NTf_2^- , OTf^-).⁷⁷ Addition of $\text{Na}[\text{IMP-R}]$ to tBuXPhosAuCl in a 1:1 mixture of DCM/MeCN generated the analogous **2** $[\text{IMP-R}]$ complexes. When performed in CD_2Cl_2 (1 mol%, RT) the [2+2] cyclisation of α -methyl styrene and phenylacetylene was compatible with $[\text{IMP-CF}_3]^-$, $[\text{IMP-NO}_2]^-$, and $[\text{IMP-CO}_2\text{Me}]^-$ anions as well as the phenylbenzimidazole-based anion $[\text{BIMP}]^-$ (Table 3). **2** $[\text{BAR}_4^{\text{F}}]$, **2** $[\text{BIMP}]$ and **2** $[\text{SbF}_6]$ showed slightly better yields and reaction rates than the **2** $[\text{IMP-R}]$ complexes (Fig. 6). Moving to toluene presents a solubility challenge for conventional gold salts; even with the lipophilic *tBuXPhos* ligand, **2** $[\text{SbF}_6]$ is completely insoluble, while **2** $[\text{BAR}_4^{\text{F}}]$ is only slightly soluble. In contrast, several of the IMP-R complexes dissolve in toluene, including **2** $[\text{IMP-H}]$, **2** $[\text{IMP-CF}_3]$, **2** $[\text{IMP-NO}_2]$ and **2** $[\text{BIMP}]$. **2** $[\text{IMP-CO}_2\text{Me}]$ is completely insoluble. **2** $[\text{IMP-H}]$ and **2** $[\text{IMP-CF}_3]$ provide good yields and rates in cyclisations run in toluene-*d*₈ (Fig. 7), while the more tightly-coordinating $[\text{IMP-NO}_2]^-$ shows decreased reactivity, and $[\text{IMP-CO}_2\text{Me}]^-$ fails entirely. Meanwhile the poorly-soluble **2** $[\text{BAR}_4^{\text{F}}]$ provides inconsistent conversions in toluene.

Table 3 Activity of complexes 2[X] in [2+2] cyclisations

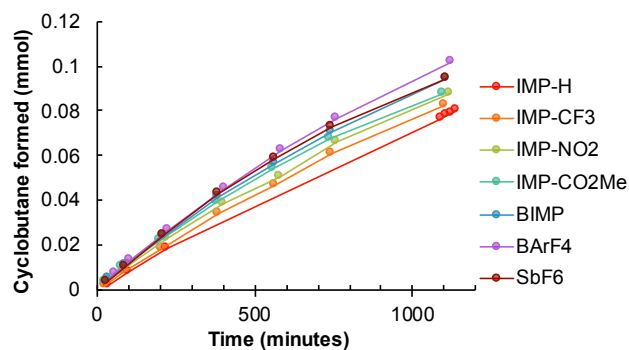
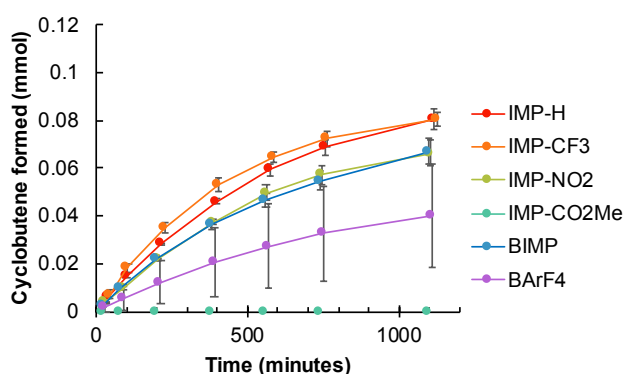
$$2[X] = L-Au-NCMe^+ X^-$$

L =

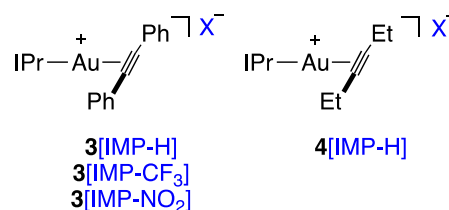
| | |
|---------------------------|-----------------------------------|
| 2[IMP-H] | 2[SbF ₆] |
| 2[IMP-CF ₃] | 2[BAr ^F ₄] |
| 2[IMP-NO ₂] | |
| 2[IMP-CO ₂ Me] | |
| 2[BIMP] | |

| Anion | % Yield in CD ₂ Cl ₂ at 18h ^a | % Yield in toluene-d ₈ at 18h ^a |
|-------------------------------|--|---|
| IMP-H | 46 | 47 |
| IMP-CF ₃ | 47 | 47 |
| IMP-NO ₂ | 46 | 37 |
| IMP-CO ₂ Me | 52 | 0 |
| BIMP | 53 | 35 |
| BAr ^F ₄ | 64 | 23 |
| SbF ₆ | 54 | - |

^a All yields are average of at least two trials.

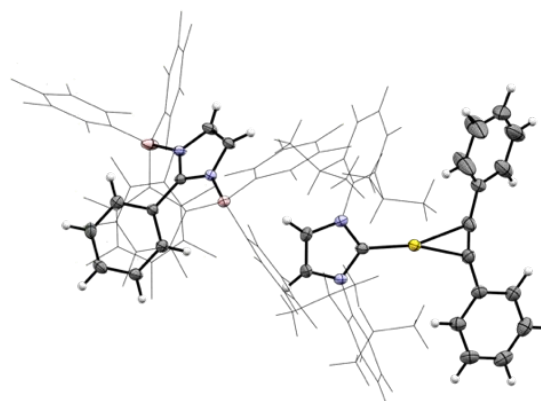
**Fig. 6** Reaction profile of [2+2] cyclisation in dichloromethane catalysed by 2[X].**Fig. 7** Reaction profile of [2+2] cyclisation in toluene catalysed by 2[X]; error bars show standard deviation of three runs.

A second series of Au complexes (Fig. 8) was prepared for the gold-catalysed hydroalkoxylation of 3-hexyne, a reaction where basic counteranions have been proposed to play active roles in catalytic mechanisms (*vide supra*). Empirical evidence reported by Zuccaccia and co-workers shows that anion identity has a marked effect on catalytic activity, even in the presence of a coordinating solvent such as methanol.^{20-22,25} We believed

**Fig. 8** Au complexes 3-4.

that the variable coordinating ability of [IMP-R]⁻ anions would allow for an exploration of the accelerating effect observed by Zuccaccia, Belanzoni and coworkers¹⁹⁻²¹ and Zhdanko and Maier.²⁴

Among the complexes prepared were series **3**. The X-ray structures of **3[IMP-H]** and **3[IMP-CF₃]** are, to our knowledge, the first of Au complexes of diphenylacetylene. These compounds proved to be thermally unstable, decomposing at -35 °C over the course of several days. In the solid-state structure of **3[IMP-H]** the C-C≡C alkyne bond angle is significantly distorted from linearity (~162°; Fig. 9). Because of their rapid decomposition at cryogenic conditions we did not consider complexes **3** further in catalytic experiments. Complex **4** was stable at room temperature but in our hands solutions became bright purple during attempts at hydroalkoxylation of 3-hexyne with methanol, suggesting the formation of gold nanoparticles; the complexes were also significantly less efficient than (IPr)Au(OTf).²³

**Fig. 9** Thermal ellipsoid plot of **3[IMP-H]**. Ellipsoids shown at 50% probability; hydrogens hidden for clarity; diisopropylphenyl and C₆F₅ substituents shown in wireframe.

In contrast, complexes **2** were much more stable and did not generate purple solutions in the hydroalkoxylation of 3-hexyne with methanol (Fig. 10). In all cases only the ketal product was observed, consistent with general acid-catalysed conversion of the intermediate vinyl ether.⁷⁹ The 2[IMP-R] complexes performed comparably to 2[BAr^F₄], suggesting [IMP-R]⁻ is compatible with the acidic conditions generated *in situ*. We note that the *t*BuXPhos catalysts react more slowly than the corresponding IPr complexes reported by Zuccaccia and coworkers.²³

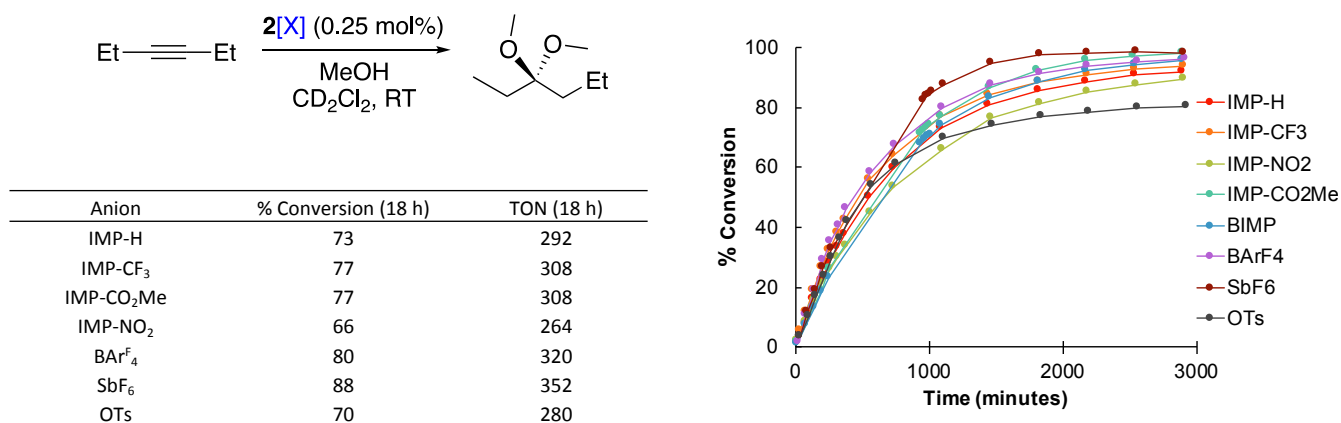


Fig. 10 Conversions, Turnover Numbers (TONs), and reaction profile of hydroalkoxylation of 3-hexyne with methanol catalysed by 2[X].

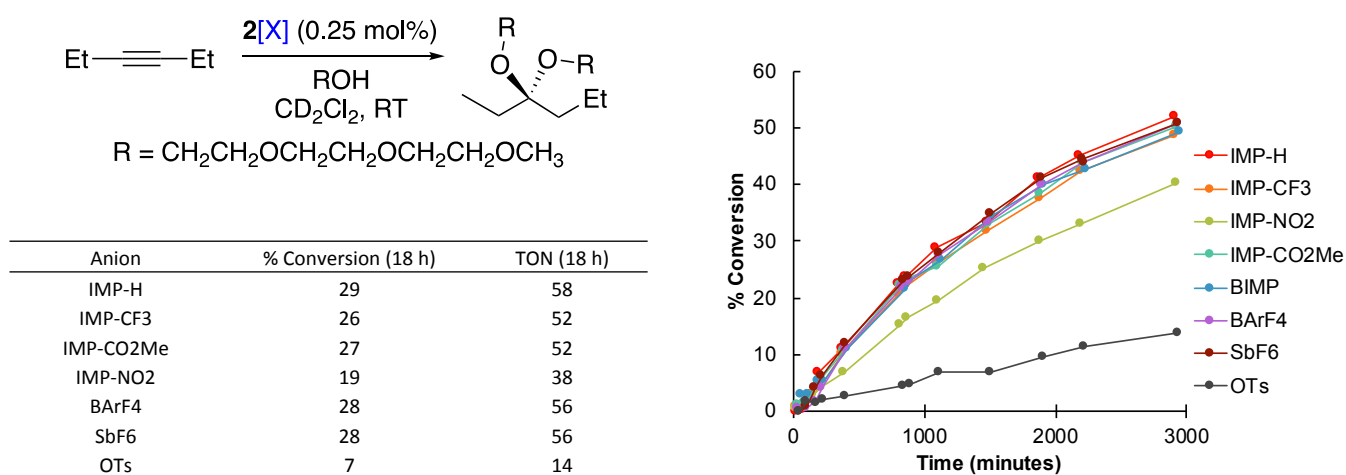


Fig. 11 Conversions, Turnover Numbers (TONs), and reaction profile of hydroalkoxylation of 3-hexyne with triethyleneglycol monomethyl ether catalysed by 2[X].

In an effort to better understand the effect of [IMP-R]⁻ anions upon catalysis, alkoxylation of 3-hexyne was attempted using the more nucleophilic triethyleneglycol monomethyl ether (Fig. 11). Consistent with previous findings of Zuccaccia and D'Amora,²¹ lower turnover numbers are observed than seen with methanol, despite the stronger nucleophilicity. SbF₆⁻ performed slightly better than [IMP-R]⁻ when using methanol as a nucleophile, but with the more challenging triethyleneglycol monomethyl ether, the rates were nearly identical, with the exception of the poorly-performing [IMP-NO₂]⁻ anion. (tBuXPhos)Au(OTs) performed worse than other weakly-coordinating anions tested, in contrast to the beneficial effect of OTs⁻ seen by Zuccaccia and co-workers for the [(IPr)Au(3-hexyne)]⁺ series of catalysts. The differences in anion influences between IPr and tBuXPhosAu complexes illustrate the complex interplay of factors – involving both ligand and counterion – that determines the efficiency of gold catalysts.²³

Discussion

Thanks to the charge-diffuse B(C₆F₅)₃ groups flanking both sides of the imidazole ring, the imidazolyl phenyl groups installed on the [IMP-R]⁻ anion scaffold retain most of the characteristics of the parent phenylimidazole molecules. The IMP anion series therefore exhibits a range of properties that can be tuned by the *para*-phenyl functionality. Based on the spectroscopy of series 1 the most weakly-coordinating is [IMP-CF₃]⁻, which mimics the coordinating ability of BArF₄⁻ and performs similarly when employed in catalytic reactions of 2. One advantage of [IMP-H]⁻ and [IMP-CF₃]⁻ is their extreme lipophilicity, as seen by the solubility of 2[IMP-CF₃]⁻ and 2[IMP-H]⁻ in toluene. The sheer size and inert nature of several lipophilic [IMP-R]⁻ anions also permitted the isolation of previously-unknown diphenylacetylene complexes 3. Like other classes of “superweak” anions, the IMP anions will likely be useful in

applications where extremely large, inert counteranions can provide stability against decomposition.

Anions $[\text{IMP-NO}_2]^-$ and $[\text{IMP-CO}_2\text{Me}]^-$ feature polar functional groups on the *para* position of the imidazolyl phenyl scaffold, enabling inner-sphere binding to transition metals in the solid-state. Based on solid-state IR measurements on $1[\text{IMP-R}]$, $[\text{IMP-NO}_2]^-$ and $[\text{IMP-CO}_2\text{Me}]^-$ are between PF_6^- and BF_4^- in coordinating ability. In solution, Pd complexes $1[\text{IMP-NO}_2]$ and $1[\text{IMP-CO}_2\text{Me}]$ appear to be fully dissociated ion pairs in CD_2Cl_2 . In Au catalysis in CD_2Cl_2 , $2[\text{IMP-CO}_2\text{Me}]$ is superior to $2[\text{IMP-NO}_2]$, and approximately as active as the more weakly-coordinating $[\text{IMP-CF}_3]^-$ and $[\text{IMP-H}]^-$.

The amide-functionalised $[\text{IMP-DMA}]^-$ and $[\text{IMP-pipA}]^-$ anions are nearly as coordinating as BF_4^- according to the solid-state IR spectra of complexes **1**. But unlike $1[\text{BF}_4]$, $1[\text{IMP-DMA}]$ and $1[\text{IMP-pipA}]$ are insoluble in DCM. The solubility of $1[\text{IMP-DMA}]$ in DMSO, and the apparent association of anion and cation in this extremely polar solvent, suggests the amide-based anions would have utility in homogeneous catalysis where very strong coordination is needed. Meanwhile, alcohol and amine-functionalised $[\text{IMP-CH}_2\text{OH}]^-$ and $[\text{IMP-CH}_2\text{NMe}_2]^-$ present difficult solubility challenges, precluding a full comparison of physical properties in organometallic venues. Nonetheless, their isolation confirms that a wide range of functional groups are compatible with the IMP scaffold.

IMP anions have proven robust and compatible with Au(I) catalysis. In the [2+2] cycloaddition reaction between alkynes and alkenes, Echavarren and coworkers⁷⁷ find the rate increased with “bulkiness and softness” of the anion, $\text{BAR}_4^- > \text{SbF}_6^- > \text{BF}_4^-$. The sterically large and lipophilic $[\text{IMP-H}]^-$ and $[\text{IMP-CF}_3]^-$ surprisingly perform somewhat worse than BAR_4^- and SbF_6^- in CD_2Cl_2 (although better in toluene due to enhanced solubility). Echavarren proposes the counteranion influences rate-determining ligand exchange to form $[\text{LAu(alkyne)}]^+$, a species in equilibrium with $[\text{LAu(MeCN)}]^+$ and an inactive digold complex. Assuming this step is rate-limiting for all counteranions examined, differences in rate may arise from other factors besides the softness of the anion. It is possible that all IMP-R anions are sufficiently “soft” to stabilise $[\text{LAu(alkyne)}]^+$ and other forces drive the equilibrium. In considering anion “softness” of the IMP scaffold, the conventional measures (size, charge diffusivity) are perhaps less critical than localised parameters (charge, steric environment) for different regions of these extremely large anions. Future work in our group will consider how to best evaluate the coordinating ability and basicity of unsymmetrical anions.

Catalysts $2[\text{IMP-R}]$ are moderately effective in alkyne hydroalkoxylation, but for the R groups investigated here (H, CF_3 , CO_2Me , NO_2) the substituent has only a negligible effect on activity. The ligand dependence of the anion effect has been observed previously²⁰ and underscores the importance of screening both anion and ligand influences during development of Au(I) catalytic methods. Ongoing work in our laboratories is exploring the use of anions featuring more basic groups in the preparation of Au complexes, since hydrogen bond acceptors are known to facilitate nucleophilic attack⁷⁹ and accelerate Au reactions where protodeauration is a turnover-limiting step.³¹

Conclusions

Weakly- to moderately-coordinating $[\text{IMP-R}]$ anions have been prepared by forming $\text{B}(\text{C}_6\text{F}_5)_3$ adducts of substituted phenylimidazolates. The coordinating ability of the anions depends on the substituent present on the phenyl ring, with more Lewis-basic functionalities resulting in stronger coordination to transition metal cations. The anions are compatible with gold catalysis, including cyclisation and alkyne functionalisation reactions. Complexes of lipophilic IMP anions $2[\text{IMP-H}]$ and $2[\text{IMP-CF}_3]$ perform particularly well in a very low dielectric medium (toluene). We envision that the IMP anion family will enable a rational tuning of anion coordinating ability and solubility – similar to steric and electronic tuning of ligands – thus allowing for enhanced control over catalytic reactions.

Experimental section

General Methods. Unless otherwise specified, all manipulations were performed under a dry N_2 atmosphere using standard Schlenk techniques or a Vacuum Atmospheres inert atmosphere glovebox. Analytical data were obtained from the CENTC Elemental Analysis Facility at the University of Rochester, funded by NSF CHE-0650456. NMR spectra were collected on Bruker Avance III 500 and 400 MHz instruments. ^1H NMR chemical shifts (δ , ppm) are referenced to residual protiosolvent resonances and ^{13}C NMR chemical shifts are referenced to the deuterated solvent peak.⁸⁰ ^{19}F (fluorobenzene) and ^{31}P (phosphoric acid) NMR chemical shifts were referenced to external standards. IR spectra were collected on a Thermo Scientific Nicolet iS5 FT-IR benchtop spectrometer with either an iD5 diamond ATR or iD1 transmission accessory. Dichloromethane (DCM), tetrahydrofuran (THF), pentane, acetonitrile, and toluene were purified using a commercial solvent purification system. All deuterated NMR solvents (Cambridge Isotope Laboratories) were dried over activated 4 Å molecular sieves for 48 h before use. Tris(pentafluorophenyl)borane ($\text{B}(\text{C}_6\text{F}_5)_3$, Boulder Scientific) was purified via sublimation (100 mtorr, 90 °C) prior to use. Chloro(dimethyl sulfide) gold (I) was purchased from Strem Chemicals. All benzonitriles, aminoacetaldehyde diethyl acetal, and tBuXPhos were purchased from Oakwood Chemicals. Sodium hydride and 2-phenylbenzimidazole were purchased from Sigma Aldrich. 2-(4-(trifluoromethyl)phenyl)imidazole, 2-(4-nitrophenyl)imidazole, and methyl 4-(imidazol-2-yl)benzoate were prepared as reported by Zhichkin and coworkers.⁸¹ Sodium tetrakis(3,5-bistrifluoromethyl)phenylborate (NaBAR_4) was prepared using the procedure of Yakelis and Bergman.¹⁶ $[\text{Pd}(\mu\text{-Cl})(\text{O}-\text{C}_9\text{H}_6\text{N})_2]$ was prepared as reported by Pregosin and coworkers.⁸² **1** was prepared as previously reported by our group.³⁴ ($^t\text{BuXPhos}$)AuCl and $[(^t\text{BuXPhos})\text{Au}(\text{NCMe})][\text{BAR}_4^-]$ were prepared using the procedures reported by Echavarren.⁷⁸ (IPr)AuCl was synthesised using the procedure reported by Nolan and coworkers.⁸³ 4-(1*H*-imidazol-2-yl)benzoic acid was synthesised according to the procedure of Hagedorn et al.⁸⁴ 4-

(1*H*-imidazol-2-yl)benzoyl chloride was synthesised according to the procedure of Webber et al.⁸⁵

Sodium 2-(4-(trifluoromethyl)phenyl)imidazolidine. In an inert atmosphere glovebox, a 16 mL vial was charged with 133 mg (0.625 mmol) 2-(4-(trifluoromethyl)phenyl)imidazole and 10 mL THF and cooled to -35 °C. The suspension was then stirred, and 15 mg (0.625 mmol) sodium hydride was added. The suspension was stirred for 20 hours and dried in vacuo. Yield 99% ¹H NMR (500 MHz, DMSO-*d*₆) δ 8.05 (d, ³*J* = 7.9 Hz, 2H, aryl), 7.48 (d, ³*J* = 8.1 Hz, 2H, aryl), 6.84 (s, 2H, imidazolyl).

Na[IMP-CF₃]. In an inert atmosphere glovebox, a 16 mL vial was charged with 140 mg (0.598 mmol) sodium 2-(4-(trifluoromethyl)phenyl)imidazolidine and 8 mL toluene and cooled to -35 °C. This solution was stirred, and 613 mg (1.197 mmol) tris(pentafluorophenyl) borane was added and stirred for 23 hours while coming to RT. The vial was removed from the glovebox and 75 mL pentane was added to precipitate the desired product as a white solid. The solid was filtered, washed with pentane, and dried in vacuo. Purification via slow diffusion of pentane into methylene chloride/THF yielded X-ray quality crystals of the product as the Na(THF)₄ salt. Yield 62%. Anal. Calc. for NaC₄₆N₂F₃₃B₂H₆·1.75C₄H₈O·0.25 CH₂Cl₂ C, 45.50 %, H, 1.47 %, N, 1.99 %, found C, 45.214 %, H, 1.829 %, N, 1.894%. ¹H NMR (500 MHz, CD₂Cl₂) δ 7.20 (s, 2H, imidazolyl), 7.02 (d, ³*J* = 8.4 Hz, 2H, aryl), 6.58 (d, ³*J* = 7.6 Hz, 2H, aryl). ¹³C NMR (126 MHz, CD₂Cl₂) δ 149.45, 147.87, 147.52, 132.62, 131.05, 130.79, 129.89, 127.13, 125.32, 125.02, 124.09. ¹⁹F NMR (471 MHz, CD₂Cl₂) δ -63.95, -126.72, -133.16, -158.80, -160.16, -164.61, -166.90. ¹¹B NMR (161 MHz, CD₂Cl₂) δ -8.24. Unit cell (XRD) monoclinic *P*, *a* = 13.103(3) Å, *b* = 27.136(5) Å, *c* = 16.187(3) Å, β = 92.560(3)°.

Sodium 2-(4-(nitro)phenyl)imidazolidine. In an inert atmosphere glovebox, a 16 mL vial was charged with 118 mg (0.625 mmol) 2-(4-(nitro)phenyl)imidazole and 10 mL THF and cooled to -35 °C. The suspension was then stirred, and 15 mg (0.625 mmol) sodium hydride was added. The suspension was stirred for 20 hours and dried in vacuo. Yield 99% ¹H NMR (500 MHz, DMSO-*d*₆) δ 8.03 (s, 4H, aryl), 6.95 (s, 2H, imidazolyl).

Na [IMP-NO₂]. In an inert atmosphere glovebox, a 16 mL vial was charged with 125 mg (0.592 mmol) sodium 2-(4-(nitro)phenyl)imidazolidine and 8 mL toluene and cooled to -35 °C. This solution was stirred, and 607 mg (1.18 mmol) tris(pentafluorophenyl) borane was added and stirred for 23 hours while coming to RT. The vial was removed from the glovebox and 75 mL pentane was added to precipitate the desired product as a light brown solid. The solid was filtered, washed with pentane, and dried in vacuo. Purification via slow diffusion of pentane into methylene chloride/THF yielded X-ray quality crystals of the product as the Na(THF)₄ salt. Yield 62%. Anal. Calc. for NaC₄₅N₃F₃₀B₂H₆·1.5C₄H₈O C, 45.60 %, H, 1.35 %, N, 3.13 %, found C, 45.418 %, H, 1.684 %, N, 3.238%. ¹H NMR (500 MHz, CD₂Cl₂) δ 7.61 (d, ³*J* = 9.1 Hz, 2H, aryl), 7.25 (d, ⁴*J* = 3.5 Hz, 2H, aryl), 6.63 (d, ³*J* = 8.1 Hz, 2H, imidazolyl). ¹³C NMR (126 MHz, CD₂Cl₂) δ 149.50, 147.64, 146.87, 146.31, 140.97, 138.98, 137.90, 136.51, 135.85, 131.12, 125.72, 122.16. ¹⁹F NMR (376 MHz, CD₂Cl₂) δ -126.21, -133.22, -158.44, -158.50, -

158.55, -159.72, -159.77, -159.82, -164.44, -164.49, -166.55 ¹¹B NMR (161 MHz, CD₂Cl₂) δ -8.07.

Sodium 2-(4-(CO₂Me)phenyl)imidazolidine. In an inert atmosphere glovebox, a 16 mL vial was charged with 202 mg (1.00 mmol) 2-(4-(CO₂Me)phenyl)imidazole and 15 mL THF and cooled to -35 °C. The suspension was then stirred, and 24 mg (1.00 mmol) sodium hydride was added. The suspension was stirred for 76 hours and dried in vacuo. Yield 99% ¹H NMR (500 MHz, DMSO-*d*₆) δ 7.97 (d, ³*J* = 8.6 Hz, 2H, aryl), 7.74 (d, ³*J* = 8.6 Hz, 2H, aryl), 6.82 (s, 2H, imidazolyl), 3.79 (s, 3H C(O)CH₃).

Na[IMP-CO₂Me]. In an inert atmosphere glovebox, a 16 mL vial was charged with 112 mg (0.50 mmol) sodium 2-(4-(CO₂Me)phenyl)imidazolidine and 8 mL toluene and cooled to -35 °C. This solution was stirred, and 512 mg (1.00 mmol) tris(pentafluorophenyl) borane was added and stirred for 26 hours. The vial was removed from the glovebox and 75 mL pentane was added to precipitate the desired product as a white solid. The solid was filtered, washed with pentane, and dried in vacuo. Purification via slow diffusion of pentane into methylene chloride/THF yielded X-ray quality crystals of the product as the Na(THF)₄ salt. Yield 56%. Anal. Calc. for NaC₄₇N₂O₂F₃₀B₂H₉·1C₄H₈O C, 46.40 %, H, 1.30 %, N, 2.12 %, found C, 46.214 %, H, 1.574 %, N, 2.056%. ¹H NMR (500 MHz, CD₂Cl₂) δ 7.32 (d, ³*J* = 8.8 Hz, 2H, aryl), 7.23 (d, ⁴*J* = 3.7 Hz, 2H, aryl), 6.51 (d, ³*J* = 7.7 Hz, 2H, imidazolyl), 3.89 (s, 3H, C(O)CH₃). ¹³C NMR (126 MHz, CD₂Cl₂) δ 169.39, 149.62, 147.54, 138.67, 137.80, 136.04, 134.64, 129.92, 129.19, 128.05, 125.38. ¹⁹F NMR (471 MHz, CD₂Cl₂) δ -125.87, -133.25, -158.70, -160.61, -164.58, -167.08. ¹¹B NMR (161 MHz, CD₂Cl₂) δ -8.12. Unit cell (XRD) triclinic, *a* = 12.2126(18) Å, *b* = 16.759(2) Å, *c* = 17.209(3) Å, α = 90.069(3)°, β = 104.596(3)°, γ = 106.610(3)°.

Sodium 2-phenylbenzimidazolidine. In an inert atmosphere glovebox, a 16 mL vial was charged with 194 mg (1.00 mmol) 2-phenylbenzimidazole and 10 mL THF and cooled to -35 °C. The suspension was then stirred, and 24 mg (1.00 mmol) sodium hydride was added. The suspension was stirred for 76 hours and dried in vacuo. Yield 99% ¹H NMR (500 MHz, DMSO-*d*₆) δ 8.22 (dd, ³*J* = 8.2, ⁴*J* = 1.2 Hz, 2H, aryl), 7.36 – 7.30 (m, 4H, aryl), 7.19 (t, ³*J* = 7.2 Hz, 1H, aryl), 6.75 (s, 2H, aryl).

Na[BIMP]. In an inert atmosphere glovebox, a 40 mL vial was charged with 223 mg (1.031 mmol) sodium 2-phenylbenzimidazolidine and 8 mL toluene and cooled to -35 °C. This solution was stirred, and 1055 mg (2.062 mmol) tris(pentafluorophenyl) borane was added and stirred for 27 hours. The vial was removed from the glovebox and 75 mL pentane was added to precipitate the desired product as a white solid. The solid was filtered, washed with pentane, and dried in vacuo. Purification via slow diffusion of pentane or HMDSO into methylene chloride/THF yielded X-ray quality crystals. Yield 79%. Anal. Calc. for NaC₄₇N₂O₂F₃₀B₂H₉·2.5C₄H₈O C, 49.85 %, H, 1.97 %, N, 2.13 %, found C, 49.951 %, H, 1.927 %, N, 2.131%. Na[BIMP] appears to exhibit complex fluxional behaviour due to hindered rotation, likely due to the increased size of the benzimidazole core versus the imidazole core of the IMP anions, and this behaviour manifests itself as broad signals in the ¹H NMR spectrum as well as with increased number of signals in the ¹⁹F spectrum. ¹H NMR (500 MHz, CD₂Cl₂) δ 7.53 (v

br s, 2H, aryl), 7.33 (v br s, 2H, aryl), 6.97 (dd, $^3J = 6.1$, $^4J = 3.2$ Hz, 4H, aryl), 6.81 (v br s, 1H, aryl). ^{13}C NMR (126 MHz, CD_2Cl_2) δ 137.83, 130.90, 128.08, 127.86, 122.90, 116.12, 114.22. ^{19}F NMR (376 MHz, CD_2Cl_2) δ -117.04, -118.92, -128.16, -129.34, -129.86, -133.91, -135.53, -136.61, -137.97, -139.02, -159.43, -159.87, -159.92, -159.97, -160.14, -160.20, -160.25, -160.89, -164.00, -164.87, -166.22, -166.99, -167.46. ^{11}B NMR (161 MHz, CD_2Cl_2) δ -7.77. Unit cell (XRD) monoclinic P, $a = 15.0906(12)$ Å, $b = 16.8592(13)$ Å, $c = 23.0499(18)$ Å, $\beta = 99.144(2)^\circ$.

4-(1H-imidazol-2-yl)-N,N-dimethylbenzamide Under ambient conditions, a 100 mL round bottom flask was charged with 10 mL dichloromethane and cooled to 0°C . 1.85 mL (8.45 mmol) of 2.0 M dimethylamine in THF was added, followed by 1.18 mL of triethylamine. The solution was stirred, and 822 mg (3.382 mmol) of 4-(1H-imidazol-2-yl)benzoyl chloride•HCl was added, resulting in HCl gas evolution. The solution was stirred for 20 minutes in the ice bath and then allowed to stir overnight at room temperature. The reaction was diluted with 100 mL dichloromethane and extracted sequentially with 15 mL saturated NaHCO_3 , brine, and NH_4Cl . The organic layer was dried over Na_2SO_4 , filtered, and concentrated to dryness under reduced pressure, resulting in a highly hygroscopic tan solid. Yield 48%. Recrystallisation via slow layer diffusion of pentane into a concentrated dichloromethane solution under N_2 atmosphere resulted in x-ray quality crystals as colourless needles. Anal. Calc. for $\text{C}_{12}\text{H}_{13}\text{N}_3\text{O} \cdot 0.1\text{C}_5\text{H}_{12} \cdot 0.1\text{CH}_2\text{Cl}_2$, 65.53 %, H, 6.28 %, N, 18.19 %, found C, 65.195 %, H, 6.544 %, N, 18.581%. ^1H NMR (500 MHz, CD_2Cl_2) δ 11.09 (s, 1H, NH), 7.82 – 7.75 (m, 2H, aryl), 7.35 (dd, $^3J = 8.2$, $^4J = 1.5$ Hz, 2H, aryl), 7.13 (s, 2H, imidazolyl), 3.09 (s, 3H, CH_3), 2.96 (s, 3H, CH_3). ^{13}C NMR (126 MHz, CD_2Cl_2) δ 171.49, 146.10, 136.33, 131.91, 127.89, 125.55, 39.75, 35.49. Unit cell (XRD) monoclinic P, $a = 15.0906(12)$ Å, $b = 16.8592(13)$ Å, $c = 23.0499(18)$ Å, $\beta = 99.144(2)^\circ$. Unit cell (XRD) orthorhombic P, $a = 7.9951(13)$ Å, $b = 14.758(2)$ Å, $c = 21.725(4)$ Å.

Na[IMP-DMA] In an inert atmosphere glovebox, a 40 mL vial was charged with 200 mg (0.930 mmol) 4-(1H-imidazol-2-yl)-N,N-dimethylbenzamide and 4 mL THF. The suspension was stirred briefly and cooled to -35°C . 23 mg (0.930 mmol) of NaH was added, and the suspension was stirred while coming to room temperature and then for an addition 15 h. The reaction was dried in vacuo, yielding a beige solid. This solid was suspended in 5 mL toluene and stirred briefly before being cooled to -35°C . 952 mg (1.860 mmol) of $\text{B}(\text{C}_6\text{F}_5)_3$ was added and the solution was stirred while coming to room temperature, and then for an additional 16 h. 30 mL of pentane was added to the reaction, resulting in a large amount of white precipitate. The reaction was removed from the glovebox, poured onto an additional 40 mL pentane, and the precipitate was filtered off, washed with hexanes, and dried in vacuo. The solid was dissolved in THF, filtered to remove insoluble impurities, and dried in vacuo. Recrystallisation *via* layer diffusion of hexanes into a concentrated THF/dichloromethane solution yielded X-ray quality crystals of the analytically pure sample; adventitious acetone was also present in the solid-state structure. Yield 41 %. Anal. Calc. for $\text{NaC}_{48}\text{H}_{12}\text{N}_3\text{B}_3\text{F}_{30}\text{O} \cdot 1.3\text{C}_4\text{H}_8\text{O}$, 47.16 %, H, 1.67 %, N, 3.10 %, found C, 46.868 %, H, 1.934 %, N, 3.284%. ^1H NMR

(500 MHz, CD_2Cl_2) δ 7.24 (d, $^3J = 4.3$ Hz, 2H, aryl), 6.69 (d, $^3J = 8.7$ Hz, 2H, aryl), 6.42 (d, $^3J = 5.6$ Hz, 2H, imidazolyl), 3.01 (s, 3H, CH_3), 2.89 (s, 3H, CH_3). ^{13}C NMR (126 MHz, CD_2Cl_2) δ 171.72, 147.56, 136.81, 130.76, 130.35, 125.23, 125.12, 39.62, 35.53. ^{19}F NMR (471 MHz, $\text{DMSO}-d_6$) δ -125.42, -133.54, -158.46, -160.17, -164.38. ^{11}B NMR (161 MHz, CD_2Cl_2) δ -8.37. Unit cell (XRD) monoclinic P, $a = 13.3526(11)$ Å, $b = 30.789(2)$ Å, $c = 16.1477(13)$ Å, $\beta = 93.240(2)^\circ$.

Na[IMP-CH₂OH] In an inert atmosphere glovebox, a 40 mL vial was charged with 300 mg (0.240 mmol) Na[IMP-CO₂Me] and 20 mL THF and stirred to dissolve. The clear, light yellow solution was cooled to -35°C and 10 mg (0.263 mmol) LiAlH_4 was added. The reaction was stirred while coming to room temperature, and then for an additional 3 days. The vial was removed from the glovebox and cooled to 0°C , at which point 1 mL H_2O , 5 drops 10% aqueous NaOH, and 15 mL diethyl ether were added sequentially. The solution was stirred while coming to room temperature and then dried over MgSO_4 . The reaction was filtered and dried in vacuo, resulting in a pure, bright white solid. Yield 79%. Analytically pure X-ray quality crystals were obtained by layering a concentrated THF solution of the product with hexanes at room temperature. Anal. Calc. for $\text{NaC}_{46}\text{N}_2\text{B}_2\text{F}_{30}\text{OH}_9 \cdot 1.45\text{C}_4\text{H}_8\text{O}$, 46.97 %, H, 1.57 %, N, 2.11 %, found C, 46.690 %, H, 1.885 %, N, 2.217 %. ^1H NMR (500 MHz, CD_2Cl_2) δ 7.21 (d, $^3J = 4.0$ Hz, 2H, aryl), 6.72 (d, $^3J = 8.5$ Hz, 2H, aryl), 6.41 (d, $^3J = 7.5$ Hz, 2H, imidazolyl), 4.54 (s, 2H, Ar- CH_2 -OH). ^{13}C NMR (126 MHz, CD_2Cl_2) δ 140.66, 139.08, 130.23, 129.73, 126.51, 125.06, 65.61. ^{19}F NMR (471 MHz, $\text{DMSO}-d_6$) δ -125.42, -133.54, -158.46, -160.17, -164.38. ^{11}B NMR (161 MHz, CD_2Cl_2) δ -8.37. Unit cell (XRD) triclinic, $a = 12.7032(13)$ Å, $b = 13.4507(13)$ Å, $c = 20.407(2)$ Å, $\alpha = 91.293(2)^\circ$, $\beta = 91.963(2)^\circ$, $\gamma = 107.760(2)^\circ$.

Na[IMP-CH₂N(Me)₂] In an inert atmosphere glovebox, a 40 mL vial was charged with 500 mg (0.3965 mmol) Na[IMP-DMA] and 30 mL THF and stirred to dissolve. The clear solution was cooled to -35°C and 17 mg (0.4360 mmol) LiAlH_4 was added. The reaction was stirred while coming to room temperature, and then for an additional 3 days. The vial was removed from the glovebox and cooled to 0°C , at which point 1 mL H_2O , 5 drops 10% aqueous NaOH, and 20 mL diethyl ether were added sequentially. The solution was stirred while coming to room temperature, and then dried over MgSO_4 . The reaction was filtered and dried in vacuo, resulting in a pure, bright white solid. Yield 80%. Analytically pure X-ray quality crystals were obtained by layering a concentrated DCM/THF solution of the product with hexanes at room temperature. Anal. Calc. for $\text{NaC}_{48}\text{N}_3\text{B}_2\text{F}_{30}\text{H}_{14} \cdot 2\text{C}_4\text{H}_8\text{O}$, 0.4 C_5H_{12} , 49.05 %, H, 2.47 %, N, 2.96 %, found C, 49.03 %, H, 2.52 %, N, 2.91 %. ^1H NMR (500 MHz, CD_2Cl_2) δ 7.25 (d, $^4J = 2.4$ Hz, 2H, aryl), 6.74 (d, $^3J = 8.4$ Hz, 2H, aryl), 6.43 (s, 2H, imidazolyl), 3.53 (s, 2H, Ar- CH_2 -N), 2.47 (d, $^3J = 9.5$ Hz, 6H, $\text{N}(\text{CH}_3)_2$). ^{13}C NMR (126 MHz, CD_2Cl_2) δ 128.95, 44.38, 22.74. ^{19}F NMR (471 MHz, CD_2Cl_2) δ -125.68, -133.30, -158.78, -160.56, -164.60, -167.16. ^{11}B NMR (161 MHz, CD_2Cl_2) δ -8.19. Unit cell (XRD) monoclinic P, $a = 12.1872(17)$ Å, $b = 19.000(3)$ Å, $c = 14.971(2)$ Å, $\beta = 111.618(3)^\circ$.

4-(1H-imidazol-2-yl)-N,N-dibutylbenzamide Under ambient conditions, a 100 mL round bottom flask was charged with 40 mL dichloromethane, 925 μL (5.5 mmol) di-*n*-butylamine, and 3

mL of triethylamine. The solution was stirred, and 1215 mg (5 mmol) of 4-(1H-imidazol-2-yl)benzoyl chloride•HCl was added, resulting in HCl gas evolution and a rapid colour change from orange/yellow to brown. The reaction was allowed to stir for 20 hours and was then diluted with 50 mL of dichloromethane. The reaction was extracted sequentially with 5 mL saturated NaHCO₃, and 5 mL brine. The organic layer was dried over Na₂SO₄, filtered, and concentrated to dryness under reduced pressure, resulting in a viscous brown oil. The oil was triturated with hexanes and dried again, resulting in a brown foam that became a solid powder when broken up. Yield 56%. HRMS (ESI) calc. for C₁₈H₂₅N₃O ([M + H]⁺): 300.2070, found 300.2077. ¹H NMR (500 MHz, CD₂Cl₂) δ 10.67 (s, 1H, NH), 7.78 (d, ³J = 8.0 Hz, 2H, aryl), 7.32 – 7.25 (m, 2H, aryl), 7.12 (s, 2H, imidazolyl), 3.53 – 3.44 (m, 2H, N-CH₂), 3.24 – 3.13 (m, 2H, N-CH₂), 1.65 (s, 2H, N-CH₂-CH₂), 1.54 – 1.34 (m, 4H, N-CH₂-CH₂ + CH₂-CH₂-CH₂), 1.17 – 1.04 (m, 2H, CH₂-CH₂-CH₂), 0.99 (t, ³J = 7.3 Hz, 3H, CH₃), 0.77 (t, J = 6.6 Hz, 3H, CH₃). ¹³C NMR (126 MHz, CD₂Cl₂) δ 171.64, 143.19, 137.28, 131.61, 130.60, 127.24, 125.58, 49.25, 44.98, 31.13, 30.04, 20.72, 20.14, 14.13, 13.80.

Na[IMP-DBA] In an inert atmosphere glovebox, a 20 mL vial was charged with 299 mg (1.00 mmol) 4-(1H-imidazol-2-yl)-N,N-dibutylbenzamide and 5 mL THF. The suspension was stirred briefly and cooled to –35 °C. 24 mg (1.00 mmol) of NaH was added, and the suspension was stirred while coming to room temperature and then for an addition 23 h. The reaction was dried in vacuo, yielding a beige solid. This solid was suspended in 8 mL toluene and stirred briefly before being cooled to –35 °C. 1024 mg (2.00 mmol) of B(C₆F₅)₃ was added and the solution was stirred while coming to room temperature, and then for an additional 18 h. 30 mL of pentane was added to the reaction, resulting in a large amount of white precipitate. The reaction was removed from the glovebox, poured onto an additional 50 mL pentane, and the precipitate was filtered off, washed with hexanes, and dried in vacuo. Yield 46%. Recrystallisation *via* layer diffusion of hexanes into a concentrated THF/dichloromethane solution yielded X-ray quality crystals of the analytically pure sample. Anal. Calc. for NaC₅₄H₂₄N₃B₂F₃₀O·1.3C₄H₈O C, 49.41 %, H, 2.41 %, N, 2.92 %, found C, 49.652 %, H, 2.400 %, N, 3.201%. ¹H NMR (500 MHz, CD₂Cl₂) δ 7.23 (d, ³J = 5.1 Hz, 2H, aryl), 6.63 (d, ³J = 8.4 Hz, 2H, aryl), 6.32 (br s, 2H, imidazolyl), 3.37 (br s, 2H, N-CH₂), 3.04 (br s, 2H, N-CH₂), 1.56 (m, 2H, N-CH₂-CH₂), 1.24 (m, 6H, N-CH₂-CH₂ + CH₂-CH₂-CH₂), 0.93 (t, ³J = 7.4 Hz, 3H, CH₃), 0.73 (t, ³J = 7.3 Hz, 3H, CH₃). ¹³C NMR (126 MHz, CD₂Cl₂) δ 171.98, 138.06, 130.98, 130.02, 129.36, 128.55, 125.11, 124.30, 49.34, 45.13, 30.99, 29.61, 20.60, 19.79, 13.98, 13.49. ¹⁹F NMR (471 MHz, CD₂Cl₂) δ -125.28, -133.47, -158.45, -160.10, -164.29, -165.76. ¹¹B NMR (161 MHz, CD₂Cl₂) δ -8.40. Unit cell (XRD) monoclinic P, *a* = 33.184(3) Å, *b* = 15.7566(14) Å, *c* = 26.172(2) Å, β = 109.217(2)°.

4-(1H-imidazol-2-yl)phenyl(piperidin-1-yl)methanone

Under ambient conditions, a 100 mL round bottom flask was charged with 30 mL dichloromethane, 434 μL (4.4 mmol) piperidine, and 2.2 mL of triethylamine. The solution was stirred, and 972 mg (4 mmol) of 4-(1H-imidazol-2-yl)benzoyl chloride•HCl was added, resulting in HCl gas evolution and a rapid colour change from orange/yellow to brown. The reaction

was allowed to stir for 15 hours and was then diluted with 50 mL of dichloromethane. The reaction was extracted sequentially with 5 mL saturated NaHCO₃, and 5 mL brine. The organic layer was dried over Na₂SO₄, filtered, and concentrated to dryness under reduced pressure, resulting in light brown solid. Yield 82%. Anal. Calc. for C₁₅H₁₇N₃O·0.1CH₂Cl₂ C, 68.75 %, H, 6.57 %, N, 15.93 %, found C, 68.360 %, H, 6.969 %, N, 16.317%. ¹H NMR (500 MHz, CD₂Cl₂) δ 11.18 (v br s, 1H, NH), 7.81 – 7.75 (dd, ³J = 8.4, ⁴J = 1.8, 2H, aryl), 7.31 (d, ³J = 8.1 Hz, 2H, aryl), 7.11 (s, 2H, imidazolyl), 3.69 (br s, 2H, N-CH₂), 3.33 (br s, 2H, N-CH₂), 1.67 (br s, 4H, N-CH₂-CH₂), 1.50 (br s, 2H, CH₂-CH₂-CH₂). ¹³C NMR (126 MHz, CD₂Cl₂) δ 170.23, 146.21, 136.32, 132.03, 127.62, 125.63, 49.15, 46.20, 43.52, 26.88, 26.05.

Na[IMP-pipA] In an inert atmosphere glovebox, a 20 mL vial was charged with 255 mg (1.00 mmol) 4-((1H-imidazol-2-yl)phenyl)(piperidin-1-yl)methanone and 5 mL THF. The suspension was stirred briefly and cooled to –35 °C. 24 mg (1.00 mmol) of NaH was added, and the suspension was stirred while coming to room temperature and then for an addition 18 h. The reaction was dried in vacuo, yielding a brown solid. This solid was suspended in 10 mL toluene and stirred briefly before being cooled to –35 °C. 1024 mg (2.00 mmol) of B(C₆F₅)₃ was added and the solution was stirred while coming to room temperature, and then for an additional 17 h. 30 mL of pentane was added to the reaction, resulting in a large amount of white precipitate. The reaction was removed from the glovebox, poured onto an additional 50 mL pentane, and the precipitate was filtered off, washed with hexanes, and dried in vacuo. Yield 77%. Recrystallisation *via* layer diffusion of hexanes into a concentrated THF/dichloromethane solution yielded X-ray quality crystals of the analytically pure sample. Anal. Calc. for NaC₅₁H₁₆N₃B₂F₃₀O·2 C₄H₈O C, 49.03 %, H, 2.23 %, N, 2.91 %, found C, 49.338 %, H, 2.435 %, N, 3.031%. ¹H NMR (500 MHz, CD₂Cl₂) δ 7.24 (d, ³J = 4.0 Hz, 2H, aryl), 6.67 (d, ³J = 8.4 Hz, 2H, aryl), 6.43 (br s, 2H, imidazolyl), 3.58 (br s, 2H, 2H, N-CH₂), 3.24 – 3.19 (m, 2H, 2H, N-CH₂), 1.68 (p, ³J = 6.2, ³J = 5.8 Hz, 2H, N-CH₂-CH₂), 1.61 (dt, ³J = 11.0, ³J = 5.8 Hz, 2H, N-CH₂-CH₂), 1.52 (p, ³J = 6.2 Hz, 2H, CH₂-CH₂-CH₂). ¹⁹F NMR (471 MHz, CD₂Cl₂) δ -125.39, -133.45, -158.48, -160.12, -164.41, -166.03. ¹¹B NMR (161 MHz, CD₂Cl₂) δ -8.82. ¹³C NMR (126 MHz, CD₂Cl₂) δ 170.06, 147.62, 141.42, 137.13, 130.48, 125.23, 124.87, 121.80, 49.23, 43.64, 26.58, 24.45. Unit cell (XRD) triclinic, *a* = 14.2164(17) Å, *b* = 14.4515(17) Å, *c* = 17.120(2) Å, α = 81.955(2)°, β = 72.302(2)°, γ = 67.813(2)°.

2-(3,5-bis(trifluoromethyl)phenyl)-1H-imidazole

This compound was synthesised using a modified version of the procedure reported by Zhichkin and coworkers.⁴⁰ Under air, a 100 mL round bottom flask was charged with 10 mL methanol and 1.68 mL (10 mmol) 3,5-bis(trifluoromethyl)benzotrile and stirred. Sodium methoxide in methanol (25%, 1 mmol) was added and the solution was stirred at room temperature for 2 h. Aminoacetaldehyde diethyl acetal (1.45 mL, 10 mmol) and 1.2 mL glacial acetic acid were then added, and the reaction was heated to 50 °C for 1 h. The reaction was cooled and diluted with 20 mL methanol, followed by addition of 5 mL 6 M HCl, and the reaction was heated to 75 °C for 5 h. After cooling, solvent was removed with a rotary evaporator, and the white residue

was taken up in 30 mL 1:1 water/diethyl ether and extracted. NaOH was added to the clear aqueous layer until it attained a pH of 10; the white precipitate that formed was filtered and dried in vacuo. The aqueous filtrate was allowed to stand overnight, during which time X-ray quality crystals grew as large colourless needles. Yield 22%. HRMS (ESI) calc. for $C_{11}H_6N_2F_6$ ($[M + H]^+$): 281.0513, found 281.0512. 1H NMR (500 MHz, DMSO- d_6) δ 13.06 (s, 1H, NH), 8.58 (s, 2H, aryl), 8.06 (s, 1H, aryl), 7.29 (s, 2H, aryl). ^{13}C NMR (126 MHz, DMSO- d_6) δ 143.21, 133.39, 131.77, 131.51, 131.25, 130.98, 124.83, 122.66, 121.43. ^{19}F NMR (471 MHz, DMSO- d_6) δ -61.55.

Na[IMP-(CF₃)₂] In an inert atmosphere glovebox, a 40 mL vial was charged with 280 mg (1.0 mmol) 2-(3,5-bis(trifluoromethyl)phenyl)-1H-imidazole and 5 mL THF. The solution was stirred briefly and cooled to -35 °C. 24 mg (1.0 mmol) of NaH was added, and the suspension was stirred while coming to room temperature and then for an addition 24 h. The reaction was dried in vacuo, yielding a white solid. This solid was suspended in 8 mL toluene and stirred briefly before being cooled to -35 °C. 1024 mg (2.0 mmol) of B(C₆F₅)₃ was added and the solution was stirred while coming to room temperature, and then for an additional 17 h. 30 mL of pentane was added to the reaction, resulting in a large amount of white precipitate. The reaction was removed from the glovebox, poured onto an additional 40 mL pentane, and the precipitate was filtered off, washed with hexanes, and dried in vacuo. The solid was purified *via* slow diffusion of hexanes into a concentrated DCM/THF solution of the product. It should be noted that the product, while solid, is very tacky and must be kept under somewhat anhydrous conditions. Yield 74 %. Anal. Calc. for NaC₄₇H₅N₂B₂F₃₆·2C₄H₈O C, 44.93 %, H, 1.44 %, N, 1.91 %, found C, 45.070 %, H, 1.615 %, N, 1.986%. 1H NMR (500 MHz, CD₂Cl₂) δ 7.61 (s, 1H, aryl), 7.27 (d, 4J = 3.5 Hz, 2H, aryl), 6.98 (s, 2H, imidazolyl). ^{13}C NMR (126 MHz, CD₂Cl₂) δ 149.45, 147.45, 145.68, 131.35, 131.13, 129.58, 125.73, 123.92, 123.01, 121.75, 108.53. ^{19}F NMR (376 MHz, CD₂Cl₂) δ -64.66, -126.24, -133.41, -158.44, -159.51, -164.37, -166.81. ^{11}B NMR (161 MHz, CD₂Cl₂) δ -8.22. Unit cell (XRD) monoclinic P, a = 15.937(3) Å, b = 25.254(4) Å, c = 18.608(3) Å, β = 106.941(3)°.

1[IMP-CF₃] In an inert atmosphere glovebox, a 4 mL vial was charged with 30 mg (0.048 mmol) of 1Cl, and 2 mL of dichloromethane and stirred to dissolve. To the bright orange solution was added 60 mg (0.048 mmol) of Na[IMP-CF₃], and the solution immediately turned bright yellow. The reaction was allowed to stir for 2.5 h and the solution was filtered through celite, layered with pentane, and stored at -35 °C to afford X-ray quality crystals as yellow needles. Yield 81%. Anal. Calc. for PdC₈₃N₅OF₃₀B₂H₄₉·CH₂Cl₂ C, 51.18 %, H, 2.56 %, N, 3.55 %, found C, 51.119 %, H, 2.720 %, N, 3.488 %. 1H NMR (500 MHz, CD₂Cl₂) δ 8.52 (d, 3J = 8.1 Hz, 1H, quinolyl), 8.22 (d, 3J = 4.8 Hz, 1H, quinolyl), 8.13 (d, 3J = 8.1 Hz, 1H, quinolyl), 7.92 (d, 3J = 7.3 Hz, 1H, quinolyl), 7.66 – 7.60 (m, 2H, quinolyl), 7.57 (t, 3J = 7.8 Hz, 2H, IPr aryl), 7.43 – 7.34 (m, 6H, IPr aryl + imidazolyl), 7.20 (s, 2H, IMP-CF₃ imidazolyl), 7.00 (d, 3J = 8.5 Hz, 2H, IMP-CF₃ aryl), 6.58 (d, 3J = 7.6 Hz, 2H, IMP-CF₃ aryl), 2.74 (hept, 3J = 6.5 Hz, 4H, CH(CH₃)₂), 1.32 (d, 3J = 6.8 Hz, 12H, CH(CH₃)₂), 1.27 (d, 3J = 6.9 Hz, 12H, CH(CH₃)₂). ^{13}C NMR (126 MHz, CD₂Cl₂) δ 147.80, 146.61,

139.89, 133.84, 131.36, 129.94, 129.64, 129.37, 125.27, 124.96, 124.04, 123.90, 29.38, 25.11, 25.05. IR (thin film, cm⁻¹): ν_{CO} 1770; IR (CH₂Cl₂, cm⁻¹): ν_{CO} 1761. Unit cell (XRD) triclinic, a = 14.1686(15) Å, b = 18.684(2) Å, c = 19.045(2) Å, α = 114.321(4)°, β = 98.469(4)°, γ = 107.830(4)°.

1[IMP-NO₂] In an inert atmosphere glovebox, a 4 mL vial was charged with 50 mg (0.079 mmol) of 1Cl and 2 mL of dichloromethane and stirred to dissolve. To the bright orange solution was added 107 mg (0.087 mmol) of Na[IMP-NO₂], and the solution immediately turned bright yellow. The reaction was allowed to stir for 16.5 h and the solution was filtered through celite and layered with pentane. This resulted in the product oiling out; layer diffusion of HMDSO into dichloromethane resulted in an analytically pure sample. Subsequent vapor diffusion of pentane into a concentrated toluene solution yielded X-ray quality crystals as yellow blocks. Yield 92%. Anal. Calc. for PdC₈₁N₆O₃F₃₀B₂H₄₉ C, 52.52 %, H, 2.67 %, N, 4.54 %, found C, 52.473 %, H, 2.364 %, N, 4.516 %. 1H NMR (500 MHz, CD₂Cl₂) δ 8.52 (d, 3J = 8.3 Hz, 1H, quinolyl), 8.21 (d, 3J = 4.6 Hz, 1H, quinolyl), 8.17 – 8.10 (m, 1H, quinolyl), 7.92 (dd, 3J = 7.3, 4J = 1.0 Hz, 1H, quinolyl), 7.65 – 7.52 (m, 6H, quinolyl + IPr aryl + IMP-NO₂ aryl), 7.39 (d, 3J = 7.8 Hz, 4H, IPr aryl), 7.36 (s, 2H, IPr imidazolyl), 7.24 (d, 3J = 4.0 Hz, 2H, IMP-NO₂ aryl), 6.59 (d, 3J = 7.9 Hz, 2H, IMP-NO₂ imidazolyl), 2.76 (hept, 3J = 6.4 Hz, 4H, CH(CH₃)₂), 1.31 (d, 3J = 6.8 Hz, 12H, CH(CH₃)₂), 1.27 (d, 3J = 6.9 Hz, 12H, CH(CH₃)₂). ^{13}C NMR (126 MHz, CD₂Cl₂) δ 175.12, 150.78, 149.37, 147.45, 146.58, 139.87, 138.97, 137.94, 135.80, 135.54, 133.85, 133.73, 131.30, 130.91, 129.61, 129.36, 125.53, 125.09, 124.95, 123.87, 122.02, 29.33, 25.13, 24.97. IR (thin film, cm⁻¹): ν_{CO} 1737; IR (CH₂Cl₂, cm⁻¹): ν_{CO} 1761. Unit cell (XRD) monoclinic P, a = 18.6043(18) Å, b = 26.890(3) Å, c = 21.779(2) Å, β = 101.862(2)°.

1[IMP-CO₂Me] In an inert atmosphere glovebox, a 4 mL vial was charged with 61 mg (0.095 mmol) of 1Cl and 2 mL of dichloromethane and stirred to dissolve. To the bright orange solution was added 100 mg (0.048 mmol) of Na[IMP-CO₂Me], and the solution immediately turned bright yellow. The reaction was allowed to stir for 0.5 h and the solution was filtered through celite, layered with pentane. Recrystallisation under air *via* vapor diffusion of hexanes into a concentrated methylene chloride solution afforded X-ray quality crystals. Yield 81%. Anal. Calc. for PdC₈₄N₅O₃F₃₀B₂H₅₁·1.5C₄H₈O C, 54.36 %, H, 3.13 %, N, 3.56 %, found C, 54.694 %, H, 3.139 %, N, 3.636 %. 1H NMR (500 MHz, CD₂Cl₂) δ 8.50 (d, 3J = 8.2 Hz, 1H, quinolyl), 8.23 (d, 3J = 4.6 Hz, 1H, quinolyl), 8.12 (d, 3J = 8.1 Hz, 1H, quinolyl), 7.91 (dd, 3J = 7.3, 4J = 1.1 Hz, 1H, quinolyl), 7.65 – 7.58 (m, 2H, quinolyl), 7.56 (m, J = 7.8 Hz, 3H, quinolyl + IPr aryl), 7.39 (d, 3J = 7.8 Hz, 4H, IPr aryl), 7.37 – 7.35 (s + d, 3J = 8.9 Hz, 2H + 2H, IPr imidazolyl + IMP-CO₂Me aryl), 7.20 (d, 4J = 3.7 Hz, 2H, IMP-CO₂Me aryl), 6.44 (d, 3J = 7.6 Hz, 2H, IMP-CO₂Me imidazolyl), 3.81 (s, 3H, C(O)CH₃), 2.76 (hept, 3J = 6.6 Hz, 4H, CH(CH₃)₂), 1.31 (d, 3J = 6.8 Hz, 12H, CH(CH₃)₂), 1.27 (d, 3J = 6.8 Hz, 12H, CH(CH₃)₂). ^{13}C NMR (126 MHz, CD₂Cl₂) δ 166.42, 150.90, 149.33, 148.25, 146.60, 139.83, 133.82, 133.28, 131.32, 129.90, 129.59, 129.49, 129.33, 128.19, 125.09, 123.90, 52.57, 35.01, 34.52, 29.33, 25.63, 25.06, 23.06, 11.60. IR (thin film, cm⁻¹): ν_{CO} 1729; IR (CH₂Cl₂, cm⁻¹): ν_{CO} 1761.

Unit cell (XRD) monoclinic P, $a = 22.722(2)$ Å, $b = 18.9379(19)$ Å, $c = 22.844(2)$ Å, $\beta = 105.759(2)^\circ$.

1[IMP-(CF₃)₂] In an inert atmosphere glovebox, a 4 mL vial was charged with 50 mg (0.0786 mmol) of **1Cl** and 1 mL of dichloromethane and stirred to dissolve. To the bright orange solution was added 110 mg (0.0825 mmol) of Na[IMP-(CF₃)₂], and the solution immediately turned bright yellow. The reaction was allowed to stir for 16 h and the solution was filtered through celite, layered with pentane, and stored at -35°C to afford X-ray quality crystals as yellow blocks. Yield 93%. Anal. Calc. for PdC₈₄N₅OF₃₆B₂H₄₈ · 0.9 CH₂Cl₂ C, 50.19 %, H, 2.47 %, N, 3.45 %, found C, 50.238 %, H, 2.502 %, N, 3.360 %. ¹H NMR (500 MHz, CD₂Cl₂) δ 8.51 (dd, ³J = 8.4, ⁴J = 1.1 Hz, 1H, quinolyl), 8.22 (d, ³J = 4.4 Hz, 1H, quinolyl), 8.12 (dd, ³J = 8.1, ⁴J = 1.0 Hz, 1H, quinolyl), 7.90 (dd, ³J = 7.3, ⁴J = 1.1 Hz, 1H, quinolyl), 7.63 – 7.53 (m, 5H, quinolyl + IPr aryl + IMP-(CF₃)₂ aryl), 7.38 (d, ³J = 7.8 Hz, 4H, IPr aryl), 7.35 (s, 2H, IPr imidazolyl), 7.25 (d, ³J = 3.8 Hz, 2H, IMP-(CF₃)₂ aryl), 6.97 (s, 2H, IMP-(CF₃)₂ imidazolyl), 2.74 (hept, ³J = 6.7 Hz, 4H), 1.31 (d, ³J = 6.8 Hz, 12H), 1.26 (d, ³J = 6.9 Hz, 12H). ¹³C NMR (126 MHz, CD₂Cl₂) δ 174.83, 150.89, 149.38, 146.60, 145.65, 139.89, 133.83, 133.75, 131.34, 131.18, 131.05, 130.00, 129.63, 129.36, 125.70, 125.65, 125.10, 124.95, 123.93, 123.90, 122.91, 121.76, 29.36, 25.12, 25.03. Solid state IR 1755 cm⁻¹, soln. state 1761 cm⁻¹. Unit cell (XRD) triclinic, $a = 13.652(5)$ Å, $b = 16.550(6)$ Å, $c = 20.994(8)$ Å, $\alpha = 112.393(7)^\circ$, $\beta = 91.470(7)^\circ$, $\gamma = 101.814(7)^\circ$.

1[IMP-DMA] In an inert atmosphere glovebox, a 4 mL vial was charged with 50 mg (0.0786 mmol) of **1Cl** and 1 mL of dichloromethane and stirred to dissolve. To the bright orange solution was added 104 mg (0.0825 mmol) of Na[IMP-DMA], and the solution immediately turned bright yellow. After less than a minute of stirring, a large amount of pale-yellow precipitate was observed. The reaction was allowed to stir for 16 h and the solution was filtered through a frit. The pale yellow solid and yellow filtrate were each dried in vacuo; NMR of each revealed that the solid was the desired product. Yield 85%. Recrystallisation of the solid from dichloromethane/acetonitrile/hexanes yielded X-ray quality crystals of the MeCN adduct. Anal. Calc. for PdC₈₇N₇O₂F₃₀B₂H₅₉ · 0.65 CH₂Cl₂ C, 52.97 %, H, 3.06 %, N, 4.93 %, found C, 53.23 %, H, 3.12 %, N, 4.65 %. ¹H NMR (500 MHz, DMSO-d₆) δ 9.60 (dd, ³J = 5.0, ⁴J = 1.5 Hz, 1H, quinolyl), 8.69 (dd, ³J = 8.3, ⁴J = 1.4 Hz, 1H, quinolyl), 8.20 (dd, ³J = 8.0, ⁴J = 1.2 Hz, 1H, quinolyl), 7.81 – 7.73 (m, 4H, quinolyl + IPr aryl), 7.71 – 7.66 (m, 1H, quinolyl), 7.39 (t, ³J = 7.7 Hz, 2H, IPr aryl), 7.30 – 7.21 (m, 6H, IPr aryl + IPr imidazolyl IMP-DMA aryl), 6.89 (d, ³J = 8.5 Hz, 2H, IMP-DMA aryl), 6.26 (s, 2H, IMP-DMA imidazolyl), 3.40 – 3.33 (m, 2H, CH(CH₃)₂), 3.10 (hept, ³J = 5.9 Hz, 2H, CH(CH₃)₂), 2.90 (s, 3H, N-CH₃), 2.78 (s, 3H, N-CH₃), 1.32 (d, ³J = 6.6 Hz, 6H, CH(CH₃)₂), 1.19 (d, ³J = 6.9 Hz, 6H, CH(CH₃)₂), 0.99 (dd, ³J = 14.1, ³J = 6.7 Hz, 12H, CH(CH₃)₂). ¹H NMR of MeCN adduct (500 MHz, CD₂Cl₂) δ 8.52 – 8.46 (m, 2H, quinolyl), 8.04 (dd, ³J = 8.1, ⁴J = 1.1 Hz, 1H, quinolyl), 7.87 (dd, ³J = 7.3, ⁴J = 1.2 Hz, 1H, quinolyl), 7.64 – 7.57 (m, 2H, quinolyl), 7.44 (t, ³J = 7.8 Hz, 2H, IPr aryl), 7.32 – 7.27 (m, 6H, IPr aryl + IPr imidazolyl), 7.19 (d, ³J = 3.5 Hz, 2H, IMP-DMA aryl), 6.77 (d, ³J = 8.7 Hz, 2H, IMP-DMA aryl), 6.36 (s, 2H, IMP-DMA imidazolyl), 3.02 (dt, ³J = 13.2, ³J = 6.4 Hz, 4H, CH(CH₃)₂), 2.79 (d,

$J = 9.8$ Hz, 6H), 2.16 (s, 3H, MeCN CH₃), 1.17 (dd, ³J = 11.9, ³J = 6.8 Hz, 24H, CH(CH₃)₂). ¹³C NMR (126 MHz, CD₂Cl₂) δ 176.76, 170.67, 150.28, 149.52, 146.61, 139.85, 135.35, 133.34, 132.31, 130.82, 129.39, 127.40, 126.44, 125.11, 124.82, 128.28, 34.53, 28.89, 26.11, 23.57, 22.75. IR (thin film, cm⁻¹): $\nu_{C=O}$ 1755 cm⁻¹, IR (CH₂Cl₂, cm⁻¹): $\nu_{C=O}$ 1761 cm⁻¹.

1[IMP-pipA] In an inert atmosphere glovebox, a 4 mL vial was charged with 50 mg (0.0786 mmol) of **1Cl** and 1 mL of dichloromethane and stirred to dissolve. To the bright orange solution was added 108 mg (0.0825 mmol) of Na[IMP-pipA], and the solution immediately turned bright yellow. After less than a minute of stirring, a large amount of pale-yellow precipitate was observed. The reaction was allowed to stir for 16 h and the solution was filtered through a frit. The pale yellow solid and yellow filtrate were each dried in vacuo; NMR of each revealed that the solid was the desired product. Yield 79%. Recrystallisation of the solid from dichloromethane/acetonitrile/hexanes yielded X-ray quality crystals of the MeCN adduct. Anal. Calc. for PdC₉₀N₇O₂F₃₀B₂H₆₃ · 1.45 C₆H₁₄ · 1.35 CH₂Cl₂ C, 54.05 %, H, 3.86 %, N, 4.43 %, found C, 54.472 %, H, 3.392 %, N, 3.949 %. ¹H NMR of MeCN adduct (500 MHz, CD₂Cl₂) δ 8.54 (br s, 1H, quinolyl), 8.52 – 8.48 (m, 1H, quinolyl), 8.04 (dd, ³J = 8.1, ⁴J = 1.1 Hz, 1H, quinolyl), 7.88 (dd, ³J = 7.3, ⁴J = 1.2 Hz, 1H, quinolyl), 7.65 – 7.57 (m, 2H, quinolyl), 7.44 (t, ³J = 7.8 Hz, 2H, IPr aryl), 7.32 – 7.27 (m, 6H, IPr aryl + IPr imidazolyl), 7.18 (d, ³J = 3.2 Hz, 2H, IMP-pipA aryl), 6.73 (d, ³J = 8.7 Hz, 2H, IMP-pipA aryl), 6.34 (br s, 2H, IMP-pipA imidazolyl), 3.43 (br s, 2H, N-CH₂), 3.09 (br s, 2H, N-CH₂), 3.02 (hept, ³J = 7.0 Hz, 4H, CH(CH₃)₂), 2.16 (s, 3H, MeCN CH₃), 1.52 (s, 2H, N-CH₂-CH₂), 1.34 (s, 4H, N-CH₂-CH₂ + CH₂-CH₂-CH₂), 1.19 (d, ³J = 6.7 Hz, 12H, CH(CH₃)₂), 1.16 (d, ³J = 6.8 Hz, 12H, CH(CH₃)₂). ¹³C NMR (126 MHz, CD₂Cl₂) δ 176.78, 169.37, 150.36, 149.55, 148.44, 141.22, 139.93, 137.19, 135.40, 132.27, 130.80, 130.10, 129.79, 129.40, 129.32, 128.54, 127.33, 126.12, 125.13, 124.82, 123.16, 35.02, 34.53, 29.45, 28.88, 26.15, 25.64, 24.68, 23.51, 22.75, 20.82, 3.51. IR (thin film, cm⁻¹): $\nu_{C=O}$ 1755 cm⁻¹, IR (CH₂Cl₂, cm⁻¹): $\nu_{C=O}$ 1761 cm⁻¹. Unit cell (MeCN adduct) (XRD) triclinic, $a = 15.857(3)$ Å, $b = 19.087(4)$ Å, $c = 19.142(4)$ Å, $\alpha = 115.371(3)^\circ$, $\beta = 106.919(3)^\circ$, $\gamma = 99.963(4)^\circ$.

2[IMP-H] In an inert atmosphere glovebox, a 4 mL vial was charged with 61 mg (0.094 mmol) (^tBuXPhos)AuCl and 2 mL of 1:1 methylene chloride:MeCN and stirred to dissolve. 123 mg (0.1036 mmol) Na[(BCF)₂(imid)] was added to the vial and the solution was stirred for 21 h. The solution was then dried in vacuo, dissolved in 2 mL of methylene chloride, filtered through celite, layered with pentane, and stored at -35°C. The product crystallised as a colourless solid, yield 68%. Anal. Calc. for AuPC₇₆N₃F₃₀B₂H₅₅ · 1.7 CH₂Cl₂ C, 47.27 %, H, 2.98 %, N, 2.13 %, found C, 47.670 %, H, 2.571 %, N, 2.012 %. ¹H NMR (500 MHz, CD₂Cl₂) δ 7.89 (td, ³J = 9.0, ³J = 8.4, ⁴J = 1.6 Hz, 1H, P-aryl), 7.67 – 7.57 (m, 2H, P-aryl), 7.36 – 7.30 (m, 1H, P-aryl), 7.16 (br s, 4H, P-aryl + IMP-H aryl), 7.04 (tt, ³J = 7.5, ⁴J = 1.1 Hz, 1H, IMP-H imidazolyl), 6.71 (t, ³J = 8.0 Hz, 2H, IMP-H aryl), 6.39 – 6.31 (m, 2H, IMP-H imidazolyl), 2.95 (hept, ³J = 7.0 Hz, 1H, Ar-CH(CH₃)₂), 2.33 (hept + s, ³J = 6.7 Hz, 5H, Ar-CH(CH₃)₂ + MeCN CH₃), 1.42 (d, ³J = 16.3 Hz, 18H, P-C(CH₃)₃), 1.33 (d, ³J = 6.9 Hz, 6H, Ar-CH(CH₃)₂), 1.26 (d, ³J = 6.8 Hz, 6H, Ar-CH(CH₃)₂), 0.93 (d, $J = 6.6$

Hz, 6H, Ar-CH(CH₃)₂). ¹³C NMR (126 MHz, CD₂Cl₂) δ 150.20, 149.57, 147.78, 135.25, 134.57, 131.98, 129.15, 128.86, 128.67, 127.98, 124.69, 124.65, 122.28, 39.15, 38.93, 34.44, 31.38, 31.34, 31.31, 26.15, 23.22. ³¹P NMR (203 MHz, CD₂Cl₂) δ 58.32.

2[IMP-CF₃]. In an inert atmosphere glovebox, a 4 mL vial was charged with 47 mg (0.0696 mmol) (^tBuXPhos)AuCl and 2 mL of 1:1 methylene chloride:MeCN and stirred to dissolve. 100 mg (0.104 mmol) Na[IMP-CF₃] was added to the vial and the solution was stirred for 17 h. The solution was then dried in vacuo, dissolved in 2 mL of methylene chloride, filtered through celite, layered with HMDSO, and stored at -35°C. The product crystallised as a colourless solid, yield 67%. Anal. Calc. for AuPC₇₇N₃F₃₃B₂H₅₄•1.5 CH₂Cl₂ C, 46.56 %, H, 2.84 %, N, 2.07 %, found C, 46.000 %, H, 2.723 %, N, 2.320%. ¹H NMR (500 MHz, CD₂Cl₂) δ 7.89 (td, ³J = 8.9, ³J = 8.4, ⁴J = 1.5 Hz, 1H, P-aryl), 7.66 – 7.57 (m, 2H, P-aryl), 7.33 (ddd, ³J = 7.3, ³J = 4.9, ⁴J = 1.8 Hz, 1H, P-aryl), 7.20 (s, 2H, IMP-CF₃ aryl), 7.17 (s, 2H, P-aryl), 7.01 (d, ³J = 8.4 Hz, 2H, IMP-CF₃ aryl), 6.58 (d, ³J = 7.7 Hz, 2H, IMP-CF₃ imidazolyl), 2.95 (hept, ³J = 6.7 Hz, 1H, Ar-CH(CH₃)₂), 2.32 (hept + s, ³J = 6.7 Hz, 5H, Ar-CH(CH₃)₂ + MeCN CH₃), 1.42 (d, ³J = 16.3 Hz, 18H, P-C(CH₃)₃), 1.33 (d, ³J = 6.9 Hz, 6H, Ar-CH(CH₃)₂), 1.26 (d, ³J = 6.8 Hz, 6H, Ar-CH(CH₃)₂), 0.93 (d, ³J = 6.6 Hz, 6H, Ar-CH(CH₃)₂). ¹³C NMR (126 MHz, CD₂Cl₂) δ 147.80, 135.27, 131.99, 129.93, 127.99, 125.28, 122.29, 39.17, 38.95, 34.45, 31.40, 31.35, 26.15, 24.34, 23.24. ³¹P NMR (202 MHz, CD₂Cl₂) δ 58.48. Unit cell (XRD) monoclinic P, *a* = 11.2277(11) Å, *b* = 21.034(2) Å, *c* = 17.1640(18) Å, β = 98.416(2)°.

2[IMP-NO₂]. In an inert atmosphere glovebox, a 4 mL vial was charged with 61 mg (0.094 mmol) (^tBuXPhos)AuCl and 2 mL of 1:1 methylene chloride:MeCN and stirred to dissolve. 128 mg (0.104 mmol) Na[IMP-NO₂] was added to the vial and the solution was stirred for 18 h. The solution was then dried in vacuo, dissolved in 2 mL of methylene chloride, filtered through celite, layered with pentane, and stored at -35°C. The product crystallised as a colourless solid, yield 69%. Anal. Calc. for AuPC₇₆N₄F₃₀B₂H₅₄O₂•0.85CH₂Cl₂, 47.41 %, H, 2.88 %, N, 2.88 %, found C, 47.851 %, H, 2.437 %, N, 3.010 %. ¹H NMR (500 MHz, CD₂Cl₂) δ 7.92 – 7.86 (m, 1H, P-aryl), 7.66 – 7.56 (m + d, ³J = 9.3, 2H + 2H, P-aryl + IMP-NO₂ aryl), 7.33 (ddd, ³J = 7.3, ³J = 4.9, ⁴J = 1.5 Hz, 1H, P-aryl), 7.24 (d, ³J = 3.7 Hz, 2H, IMP-NO₂ aryl), 7.16 (s, 2H, P-aryl), 6.60 (d, ³J = 8.0 Hz, 2H, IMP-NO₂ imidazolyl), 2.95 (hept, ³J = 7.0 Hz, 1H, Ar-CH(CH₃)₂), 2.33 (hept + s, ³J = 6.7 Hz, 3H + 2H, Ar-CH(CH₃)₂ + MeCN CH₃), 1.44 (s, 9H, P-C(CH₃)₃), 1.40 (s, 9H, P-C(CH₃)₃), 1.33 (d, ³J = 6.9 Hz, 6H, Ar-CH(CH₃)₂), 1.26 (d, ³J = 6.8 Hz, 6H, Ar-CH(CH₃)₂), 0.93 (d, ³J = 6.6 Hz, 6H, Ar-CH(CH₃)₂). ¹³C NMR (126 MHz, CD₂Cl₂) δ 150.20, 147.78, 147.39, 146.65, 134.58, 132.00, 130.86, 127.98, 126.00, 125.55, 125.51, 122.28, 122.04, 39.16, 38.93, 34.44, 31.38, 31.34, 26.14, 24.33, 23.23. ³¹P NMR (202 MHz, CD₂Cl₂) δ 58.46.

2[IMP-CO₂Me]. In an inert atmosphere glovebox, a 4 mL vial was charged with 50 mg (0.0803 mmol) (^tBuXPhos)AuCl, and 2 mL of 1:1 methylene chloride:MeCN and stirred to dissolve. 100 mg (0.104 mmol) Na[IMP-CO₂Me] was added to the vial and the solution was stirred for 24 h. The solution was then dried in vacuo, dissolved in 2 mL of methylene chloride, filtered through celite, layered with pentane, and stored at -35°C. The product crystallised as a colourless solid, yield 51%. Anal. Calc. for

AuPC₇₈N₃F₃₀B₂O₂H₅₄ C, 49.63 %, H, 3.04 %, N, 2.23 %, found C, 49.614 %, H, 3.077 %, N, 2.089%. ¹H NMR (500 MHz, CD₂Cl₂) δ 7.92 – 7.86 (m, 1H, P-aryl), 7.61 (dddd, ³J = 15.0, ³J = 7.4, ³J = 5.4, ⁴J = 3.7 Hz, 2H, P-aryl), 7.38 – 7.31 (d + m, ³J = 9.08, 2H + 1H, IMP-CO₂Me aryl + P-aryl), 7.20 (d, ³J = 3.6 Hz, 2H, IMP-CO₂Me aryl), 7.16 (s, 2H, P-aryl), 6.44 (s, 2H, IMP-CO₂Me imidazolyl), 3.84 (s, 3H, IMP-CO₂CH₃), 2.94 (hept, ³J = 7.0 Hz, 1H, Ar-CH(CH₃)₂), 2.33 (hept + s, ³J = 6.3 Hz, 2H + 3H, Ar-CH(CH₃)₂ + MeCN CH₃), 1.42 (d, ³J = 16.3 Hz, 18H, P-C(CH₃)₃), 1.33 (d, ³J = 6.9 Hz, 6H, Ar-CH(CH₃)₂), 1.26 (d, ³J = 6.8 Hz, 6H, Ar-CH(CH₃)₂), 0.93 (d, ³J = 6.6 Hz, 6H, Ar-CH(CH₃)₂). ¹³C NMR (126 MHz, CD₂Cl₂) δ 147.77, 135.24, 131.98, 128.15, 122.28, 52.61, 39.15, 34.44, 31.33, 26.14, 24.33, 23.22. ³¹P NMR (203 MHz, CD₂Cl₂) δ 58.32. Unit cell (XRD) monoclinic P, *a* = 11.4352(19) Å, *b* = 20.494(3) Å, *c* = 17.462(3) Å, β = 98.794(4)°.

2[BIMP]. In an inert atmosphere glovebox, a 4 mL vial was charged with 61 mg (0.094 mmol) (^tBuXPhos)AuCl and 2 mL of 1:1 methylene chloride:MeCN and stirred to dissolve. 129 mg (0.1036 mmol) Na[BIMP] was added to the vial and the solution was stirred for 24 h. The solution was then dried in vacuo, dissolved in 2 mL of methylene chloride, filtered through celite, layered with pentane, and stored at -35°C. The product crystallised as a colourless solid, yield 83%. Anal. Calc. for AuPC₈₀N₃F₃₀B₂H₅₉•0.5CH₂Cl₂ C, 50.24 %, H, 3.14 %, N, 2.18 %, found C, 50.528 %, H, 2.965 %, N, 2.154. ¹H NMR (500 MHz, CD₂Cl₂) δ 7.92 – 7.87 (m, 1H, P-aryl), 7.67 – 7.57 (m, 2H, P-aryl), 7.53 (br s, 2H, BIMP aryl), 7.33 (ddd, ³J = 7.3, ³J = 3.4, ⁴J = 1.6 Hz, 4H, BIMP aryl), 7.17 (s, 2H, P-aryl), 6.96 (m, 2H, P-aryl + BIMP aryl), 6.80 (br s, 1H, BIMP aryl), 2.94 (hept, ³J = 7.2 Hz, 1H, Ar-CH(CH₃)₂), 2.40 – 2.19 (hept + s, ³J = 6.3 Hz, 5H, Ar-CH(CH₃)₂ + MeCN CH₃), 1.42 (d, ³J = 16.3 Hz, 18H, P-C(CH₃)₃), 1.33 (d, ³J = 6.9 Hz, 6H, Ar-CH(CH₃)₂), 1.26 (d, ³J = 6.8 Hz, 6H, Ar-CH(CH₃)₂), 0.93 (d, ³J = 6.6 Hz, 6H, Ar-CH(CH₃)₂). ¹³C NMR (126 MHz, CD₂Cl₂) δ 180.71, 150.23, 147.81, 137.88, 135.22, 134.59, 132.02, 127.93, 122.90, 122.30, 116.13, 39.18, 38.95, 31.36, 26.16, 24.34, 23.24. ³¹P NMR (202 MHz, CD₂Cl₂) δ 58.48. Unit cell (XRD) monoclinic P, *a* = 11.2277(11) Å, *b* = 21.034(2) Å, *c* = 17.1640(18) Å, β = 98.416(2)°. Unit cell (XRD) triclinic, *a* = 15.447(3) Å, *b* = 17.053(3) Å, *c* = 18.040(3) Å, α = 67.410(3)°, β = 82.920(4)°, γ = 84.125(4)°.

3[IMP-H]. In an inert atmosphere glovebox, a 4 mL vial was charged with 26 mg (0.0425 mmol) IPrAuCl, 60 mg (0.319 mmol) diphenylacetylene, and 60 mg (0.04675 mmol) Li[IMP-H]. Methylene chloride (2 mL) was added and the reaction immediately began to turn purple, likely due to formation of gold nanoparticles. The reaction was stirred for 7 minutes, at which time it was filtered through celite, layered with pentane, and placed in the freezer, resulting in the formation of colourless X-ray quality crystals. Yield 45%. Anal. Calc. for AuC₈₆N₄F₃₀B₂H₅₇•2 CH₂Cl₂ C, 50.22 %, H, 2.92 %, N, 2.66 %, found C, 50.397 %, H, 2.522 %, N, 2.683. ¹H NMR (500 MHz, CD₂Cl₂) δ 7.66 (t, ³J = 7.8 Hz, 2H, IPr aryl), 7.49 (t, ³J = 8.2 Hz, 2H, diphenylacetylene aryl), 7.45 (s, 2H, IPr imidazolyl), 7.36 (d, ³J = 7.8 Hz, 4H, IPr aryl), 7.27 (t, ³J = 7.9 Hz, 4H, diphenylacetylene aryl), 7.17 (d, ⁴J = 2.9 Hz, 2H, IMP-H aryl), 7.06 – 7.01 (m, 1H, IMP-H aryl), 6.94 – 6.89 (m, 4H, diphenylacetylene aryl), 6.71 (t, ³J = 8.0 Hz, 2H, IMP-H aryl), 6.36 (d, ³J = 7.4 Hz, 2H, IMP-H

imidazolyl), 2.48 (hept, $^3J = 6.9$ Hz, 4H, $CH(CH_3)_2$), 1.24 (d, $^3J = 6.9$ Hz, 12H, $CH(CH_3)_2$), 1.13 (d, $^3J = 6.9$ Hz, 12H, $CH(CH_3)_2$). ^{13}C NMR (126 MHz, CD_2Cl_2) δ 146.27, 133.23, 132.37, 132.29, 132.06, 129.77, 129.17, 128.66, 127.40, 125.28, 125.20, 117.45, 89.81, 29.31, 24.67, 24.14. Unit cell (XRD) triclinic, $a = 13.708(2)$ Å, $b = 18.136(3)$ Å, $c = 18.494(3)$ Å, $\alpha = 113.739(3)^\circ$, $\beta = 97.758(3)^\circ$, $\gamma = 99.532(3)^\circ$.

3[IMP-CF₃]. In an inert atmosphere glovebox, a 4 mL vial was charged with 50 mg (0.08 mmol) IPrAuCl, 72 mg (0.40 mmol) diphenylacetylene, and 100 mg (0.08 mmol) Na[IMP-CF₃]. Methylene chloride (2 mL) was added and the reaction immediately began to turn purple, likely due to formation of gold nanoparticles. The reaction was stirred for 2 minutes, at which time it was filtered through celite, layered with pentane, and placed in the freezer, resulting in the formation of colourless X-ray quality crystals. Yield 96%. Anal. Calc. for $Au_{C_{87}N_4F_{33}B_2H_{56}} \cdot 0.5 C_5H_{12}$ C, 52.72 %, H, 2.82 %, N, 2.80 %, found C, 52.891 %, H, 2.860 %, N, 2.877. 1H NMR (500 MHz, CD_2Cl_2) δ 7.66 (t, $^3J = 7.8$ Hz, 2H, IPr aryl), 7.49 (t, $^3J = 8.2$ Hz, 2H, diphenylacetylene aryl), 7.45 (s, 2H, IPr imidazolyl), 7.36 (d, $^3J = 7.8$ Hz, 4H, IPr aryl), 7.27 (t, $^3J = 7.9$ Hz, 4H, diphenylacetylene aryl), 7.19 (d, $^4J = 2.6$ Hz, 2H, IMP-CF₃ aryl), 7.00 (d, $^3J = 8.4$ Hz, 2H, IMP-CF₃ aryl), 6.94 – 6.90 (m, 4H, diphenylacetylene aryl), 6.58 (d, $^3J = 7.9$ Hz, 2H, IMP-CF₃ imidazolyl), 2.48 (hept, $^3J = 6.9$ Hz, 4H, $CH(CH_3)_2$), 1.24 (d, $^3J = 6.9$ Hz, 12H, $CH(CH_3)_2$), 1.13 (d, $^3J = 6.9$ Hz, 12H, $CH(CH_3)_2$). ^{13}C NMR (126 MHz, CD_2Cl_2) δ 146.27, 133.38, 132.30, 129.77, 125.20, 73.85, 29.32, 24.68, 24.17. Unit cell (XRD) triclinic, $a = 15.320(11)$ Å, $b = 18.411(14)$ Å, $c = 19.587(18)$ Å, $\alpha = 62.891(19)^\circ$, $\beta = 67.043(13)^\circ$, $\gamma = 89.683(14)^\circ$.

3[IMP-NO₂]. In an inert atmosphere glovebox, a 4 mL vial was charged with 50 mg (0.08 mmol) IPrAuCl, 72 mg (0.40 mmol) diphenylacetylene, and 99 mg (0.08 mmol) Na[IMP-NO₂]. Methylene chloride (2 mL) was added and the reaction immediately began to turn purple, likely due to formation of gold nanoparticles. The reaction was stirred for 2 minutes, at which time it was filtered through celite, layered with pentane, and placed in the freezer, resulting in the formation of colourless crystals. Yield 72%. Anal. Calc. for $Au_{C_{86}N_5F_{30}B_2H_{56}O_2}$ C, 52.17 %, H, 2.85 %, N, 3.54 %, found C, 52.389 %, H, 2.757 %, N, 3.666. 1H NMR (500 MHz, CD_2Cl_2) δ 7.67 (d, $^3J = 7.9$ Hz, 2H, IPr aryl), 7.58 (d, $^3J = 9.1$ Hz, 2H, IMP-NO₂ aryl), 7.50 (t, $^3J = 7.0$ Hz, 2H, diphenylacetylene aryl), 7.46 (s, 2H, IPr imidazolyl), 7.36 (d, $^3J = 7.8$ Hz, 4H, IPr aryl), 7.30 – 7.24 (m, 4H, diphenylacetylene aryl), 7.23 (d, $^3J = 4.1$ Hz, 2H, IMP-NO₂ aryl), 6.94 – 6.90 (m, 4H, diphenylacetylene aryl), 6.58 (d, $^3J = 8.0$ Hz, 2H, IMP-NO₂ imidazolyl), 2.48 (hept, $^3J = 7.0$ Hz, 4H, $CH(CH_3)_2$), 1.24 (d, $^3J = 6.9$ Hz, 12H, $CH(CH_3)_2$), 1.13 (d, $^3J = 6.9$ Hz, 12H, $CH(CH_3)_2$). ^{13}C NMR (126 MHz, CD_2Cl_2) δ 175.07, 146.27, 132.30, 130.79, 129.77, 125.20, 121.99, 29.32, 24.68, 24.17.

4[IMP-H]. In an inert atmosphere glovebox, a 4 mL vial was charged with 50 mg (0.08 mmol) IPrAuCl, 14 μ L (0.12 mmol) 3-hexyne, and 2 mL of dichloromethane, and stirred to dissolve. Li[IMP-H] (106 mg, 0.09 mmol) was added, and the reaction immediately turned purple, indicating the formation of gold nanoparticles. The reaction was stirred for half an hour, filtered through celite, layered with pentane, and placed in the glovebox freezer, resulting in the formation of colourless X-ray

quality crystals. Yield 90%. Anal. Calc. for $Au_{C_{78}N_4F_{30}B_2H_{54}}$ C, 51.03 %, H, 2.96 %, N, 3.05 %, found C, 50.920 %, H, 2.809 %, N, 2.970. 1H NMR (500 MHz, CD_2Cl_2) δ 7.58 (t, $^3J = 7.8$ Hz, 2H, IPr aryl), 7.44 (s, 2H, IPr imidazolyl), 7.38 (d, $^3J = 7.8$ Hz, 4H, IPr aryl), 7.17 (d, $^4J = 2.8$ Hz, 2H, IMP-H aryl), 7.05 – 7.01 (m, 1H, IMP-H aryl), 6.71 (t, $^3J = 8.0$ Hz, 2H, IMP-H aryl), 6.36 (d, $^3J = 7.2$ Hz, 2H, IMP-H imidazolyl), 2.51 (hept, $^3J = 7.0$ Hz, 4H, $CH(CH_3)_2$), 2.25 – 2.18 (m, 4H, $C\equiv C-CH_2$), 1.28 (dd, $^3J = 9.3$, $^3J = 6.9$ Hz, 24H, $CH(CH_3)_2$), 0.61 (t, $J = 7.5$ Hz, 6H, $C\equiv C-CH_2-CH_3$). Unit cell (XRD) monoclinic P, $a = 12.184(6)$ Å, $b = 19.349(10)$ Å, $c = 33.546(17)$ Å, $\beta = 96.835(9)^\circ$.

(^tBuXPhos)AuOTs. In an inert atmosphere glovebox, a 4 mL vial was charged with 53 mg (0.081 mmol) (^tBuXPhos)AuCl and 1 mL of methylene chloride and stirred to dissolve. 25 mg (0.089 mmol) AgOTs was added to the vial and the reaction was stirred for 17 hours. The solution was filtered through celite and layered with pentane, but the resulting product is too soluble to recrystallise in this method. The solution was dried in vacuo, and was determined to be pure by NMR, yield 90%. Anal. Calc. for $Au_{PC_{80}N_3F_{30}B_2H_{59}}$ C, 54.54 %, H, 6.61 %, N, 0 %, found C, 54.371 %, H, 6.391 %, N, 0.018. 1H NMR (500 MHz, CD_2Cl_2) δ 7.87 (td, $^3J = 8.1$, $^4J = 1.4$ Hz, 1H, P-aryl), 7.64 (d, $^3J = 8.1$ Hz, 2H, OTs aryl), 7.57 – 7.48 (m, 2H, P-aryl), 7.34 – 7.30 (m, 1H, P-aryl), 7.18 (d, $^3J = 8.0$ Hz, 2H, OTs aryl), 7.06 (s, 2H, P-aryl), 2.78 (hept, $^3J = 6.8$ Hz, 1H, Ar- $CH(CH_3)_2$), 2.36 (s, 3H, OTs CH_3), 2.29 (hept, $^3J = 6.6$ Hz, 2H, Ar- $CH(CH_3)_2$), 1.36 (s, 9H, P- $C(CH_3)_3$), 1.33 (s, 9H, P- $C(CH_3)_3$), 1.24 (dd, $^3J = 13.5$, $^3J = 6.9$ Hz, 12H, Ar- $CH(CH_3)_2$), 0.90 (d, $^3J = 6.6$ Hz, 6H, Ar- $CH(CH_3)_2$). ^{13}C NMR (126 MHz, CD_2Cl_2) δ 150.41, 148.34, 146.51, 135.10, 134.40, 130.95, 129.06, 127.02, 126.69, 121.94, 38.77, 38.54, 34.50, 31.26, 26.35, 24.07, 22.98, 21.44. ^{31}P NMR (202 MHz, CD_2Cl_2) δ 57.19.

General procedure for [2+2] cycloadditions. An 1800 μ L stock solution of 0.00169 mmol [Au][X] and 51 mg (0.3 mmol) of 1,3,5-trimethoxybenzene (internal standard) was prepared in an inert atmosphere glovebox. 44 μ L (0.338 mmol) α -methylstyrene and 19 μ L (0.169 mmol) phenyl acetylene were each added to three NMR tubes. 600 μ L of catalyst stock solution was then added to each tube. The tubes were capped, shaken, and removed from the glovebox, and spectra were recorded at regular intervals. Yields are calculated based on ratios of integrations of product versus internal standard.

General procedure for alkyne hydroalkoxylations. Gold catalyst (0.0044 mmol) and 1,3,5-trimethoxybenzene (7 mg, 0.044 mmol) were weighed into vials in an inert atmosphere glovebox, capped, and removed. To each vial was added 400 μ L CD_2Cl_2 , 100 μ L (0.88 mmol) 3-hexyne, and 72 μ L (1.76 mmol) MeOH sequentially. The vials were capped and shaken, and the solutions were transferred to NMR tubes. Spectra were recorded at regular intervals and yields were calculated based on ratios of integrations of product versus internal standard.

Conflicts of interest

There are no conflicts to declare.

Acknowledgements

This work was supported in part by the National Science Foundation (CHE-1565721). Acknowledgment is made to the Donors of the American Chemical Society Petroleum Research Fund for partial support of this research. Support of the NMR facility at Temple University by a CURE grant from the Pennsylvania Department of Health is gratefully acknowledged. The authors thank Boulder Scientific for a gift of B(C₆F₅)₃ and Prof. Michael J. Zdilla for assistance with X-ray crystallography.

Notes and references

- I. Crossing and I. Raabe, *Angew. Chem. Int. Ed.*, 2004, **43**, 2066-2090.
- I. M. Riddlestone, A. Kraft, J. Schaefer and I. Crossing, *Angew. Chem. Int. Ed.*, 2018, **57**, 13982-14024.
- S. H. Strauss, *Chem. Rev.*, 1993, **93**, 927-942.
- C. A. Reed, *Acc. Chem. Res.*, 1998, **31**, 133-139.
- C. A. Reed, *Acc. Chem. Res.*, 2010, **43**, 121-128.
- M. Brookhart, B. Grant and A. F. Volpe, *Organometallics*, 1992, **11**, 3920-3922.
- W. Beck and K. Suenkel, *Chem. Rev.*, 1988, **88**, 1405-1421.
- E. Y.-X. Chen and T. J. Marks, *Chem. Rev.*, 2000, **100**, 1391-1434.
- S. Antoniotti, V. Dalla and E. Duñach, *Angew. Chem. Int. Ed.*, 2010, **49**, 7860-7888.
- D. A. Evans, J. A. Murry, P. von Matt, R. D. Norcross and S. J. Miller, *Angew. Chem. Int. Ed.*, 1995, **34**, 798-800.
- A. Macchioni, *Chem. Rev.*, 2005, **105**, 2039-2074.
- P. S. Pregosin, P. G. A. Kumar and I. Fernández, *Chem. Rev.*, 2005, **105**, 2977-2998.
- E. Molinos, S. K. Brayshaw, G. Kociok-Kohn and A. S. Weller, *Dalton Trans.*, 2007, 4829-4844.
- G. L. Moxham, T. M. Douglas, S. K. Brayshaw, G. Kociok-Köhn, J. P. Lowe and A. S. Weller, *Dalton Trans.*, 2006, 5492-5505.
- H. Nishida, N. Takada, M. Yoshimura, T. Sonoda and H. Kobayashi, *Bull. Chem. Soc. Jpn.*, 1984, **57**, 2600-2604.
- N. A. Yakelis and R. G. Bergman, *Organometallics*, 2005, **24**, 3579-3581.
- W. E. Geiger and F. Barrière, *Acc. Chem. Res.*, 2010, **43**, 1030-1039.
- E. Y. X. Chen and S. J. Lancaster, in *Comprehensive Inorganic Chemistry II (Second Edition)*, eds. J. Reedijk and K. Poeppelmeier, Elsevier, Amsterdam, 2013, pp. 707-754.
- L. D'Amore, G. Ciancaleoni, L. Belpassi, F. Tarantelli, D. Zuccaccia and P. Belanzoni, *Organometallics*, 2017, **36**, 2364-2376.
- G. Ciancaleoni, L. Belpassi, D. Zuccaccia, F. Tarantelli and P. Belanzoni, *ACS Catal.*, 2015, **5**, 803-814.
- M. Trinchillo, P. Belanzoni, L. Belpassi, L. Biasiolo, V. Busico, A. D'Amora, L. D'Amore, A. Del Zotto, F. Tarantelli, A. Tuzi and D. Zuccaccia, *Organometallics*, 2016, **35**, 641-654.
- D. H. Phan, B. Kim and V. M. Dong, *J. Am. Chem. Soc.*, 2009, **131**, 15608-15609.
- L. Biasiolo, M. Trinchillo, P. Belanzoni, L. Belpassi, V. Busico, G. Ciancaleoni, A. D'Amora, A. Macchioni, F. Tarantelli and D. Zuccaccia, *Chem. Eur. J.*, 2014, **20**, 14594-14598.
- A. Zhdanko and M. E. Maier, *ACS Catal.*, 2014, **4**, 2770-2775.
- P. W. Davies and N. Martin, *Org. Lett.*, 2009, **11**, 2293-2296.
- J. Schießl, J. Schulmeister, A. Doppiu, E. Wörner, M. Rudolph, R. Karch and A. S. K. Hashmi, *Adv. Synth. Catal.*, 2018, **360**, 2493-2502.
- Z. Lu, J. Han, O. E. Okoromoba, N. Shimizu, H. Amii, C. F. Tormena, G. B. Hammond and B. Xu, *Org. Lett.*, 2017, **19**, 5848-5851.
- R. M. P. Veenboer, A. Collado, S. Dupuy, T. Lebl, L. Falivene, L. Cavallo, D. B. Cordes, A. M. Z. Slawin, C. S. J. Cazin and S. P. Nolan, *Organometallics*, 2017, **36**, 2861-2869.
- B. Ranieri, I. Escofet and A. M. Echavarren, *Org. Biomol. Chem.*, 2015, **13**, 7103-7118.
- M. Jia and M. Bandini, *ACS Catal.*, 2015, **5**, 1638-1652.
- Z. Lu, G. B. Hammond and B. Xu, *Acc. Chem. Res.*, 2019, **52**, 1275-1288.
- G. L. Hamilton, E. J. Kang, M. Mba and F. D. Toste, *Science*, 2007, **317**, 496-499.
- R. J. Phipps, G. L. Hamilton and F. D. Toste, *Nat. Chem.*, 2012, **4**, 603-614.
- D. I. Wozniak, W. A. Sabbers, K. C. Weerasiri, L. V. Dinh, J. L. Quenzer, A. J. Hicks and G. E. Dobreiner, *Organometallics*, 2018, **37**, 2376-2385.
- A. Macchioni, C. Zuccaccia, E. Clot, K. Gruet and R. H. Crabtree, *Organometallics*, 2001, **20**, 2367-2373.
- M.-C. Chen, J. A. S. Roberts and T. J. Marks, *J. Am. Chem. Soc.*, 2004, **126**, 4605-4625.
- R. H. Crabtree, *The Organometallic Chemistry of the Transition Metals*, John Wiley & Sons, Inc., Hoboken, NJ, 6 edn., 2014.
- M. R. Rosenthal, *J. Chem. Educ.*, 1973, **50**, 331.
- H. G. Mayfield and W. E. Bull, *J. Chem. Soc. A*, 1971, 2279-2281.
- D. V. Peryshkov and S. H. Strauss, *Inorg. Chem.*, 2017, **56**, 4072-4083.
- A. M. Spokoyny, *Pure Appl. Chem.*, 2013, **85**, 903-919.
- S. P. Fisher, A. W. Tomich, S. O. Lovera, J. F. Kleinsasser, J. Guo, M. J. Asay, H. M. Nelson and V. Lavallo, *Chem. Rev.*, 2019, **119**, 8262-8290.
- C. Douvris and J. Michl, *Chem. Rev.*, 2013, **113**, PR179-PR233.
- Z. Jiang, Y. p. Liu, Y. Shao, P. Zhao, J. Yuan and H. Wang, *Polym. Int.*, 2019, **68**, 1566-1569.
- E. Clot, *Eur. J. Inorg. Chem.*, 2009, **2009**, 2319-2328.
- R. Díaz-Torres and S. Alvarez, *Dalton Trans.*, 2011, **40**, 10742-10750.
- A. Macchioni, G. Ciancaleoni, C. Zuccaccia and D. Zuccaccia, *Chem. Soc. Rev.*, 2008, **37**, 479-489.
- P. S. Pregosin, *Pure Appl. Chem.*, 2009, **81**, 615.
- K. E. Aldrich, B. S. Billow, D. Holmes, R. D. Bemowski and A. L. Odom, *Organometallics*, 2017, **36**, 1227-1237.
- J. C. Thomas and J. C. Peters, *J. Am. Chem. Soc.*, 2001, **123**, 5100-5101.
- Y. Sun, R. E. v. H. Spence, W. E. Piers, M. Parvez and G. P. A. Yap, *J. Am. Chem. Soc.*, 1997, **119**, 5132-5143.
- J. F. Kleinsasser, E. D. Reinhart, J. Estrada, R. F. Jordan and V. Lavallo, *Organometallics*, 2018, **37**, 4773-4783.
- Y. Wang, B. Quillian, P. Wei, C. S. Wannere, Y. Xie, R. B. King, H. F. Schaefer, P. V. Schleyer and G. H. Robinson, *J. Am. Chem. Soc.*, 2007, **129**, 12412-12413.
- M. Sircoglou, G. Bouhadir, N. Saffon, K. Miqueu and D. Bourissou, *Organometallics*, 2008, **27**, 1675-1678.
- J. C. Axtell, K. O. Kirlikovali, P. I. Djurovich, D. Jung, V. T. Nguyen, B. Munekiyo, A. T. Royappa, A. L. Rheingold and A. M. Spokoyny, *J. Am. Chem. Soc.*, 2016, **138**, 15758-15765.
- Y. Kim and R. F. Jordan, *Organometallics*, 2011, **30**, 4250-4256.
- D. Stasko and C. A. Reed, *J. Am. Chem. Soc.*, 2002, **124**, 1148-1149.
- E. S. Stoyanov, K. C. Kim and C. A. Reed, *J. Am. Chem. Soc.*, 2006, **128**, 8500-8508.
- J. C. Smith, K. Ma, W. E. Piers, M. Parvez and R. McDonald, *Dalton Trans.*, 2010, **39**, 10256-10263.
- I. Crossing, *Chem. Eur. J.*, 2001, **7**, 490-502.
- B. F. Straub, M. Wrede, K. Schmid and F. Rominger, *Eur. J. Inorg. Chem.*, 2010, **2010**, 1907-1911.

- 62 T. Söhner, F. Braun, L. C. Over, S. Mehlhose, F. Rominger and B. F. Straub, *Green Chem.*, 2014, **16**, 4696-4707.
- 63 M. H. Hannant, J. A. Wright, S. J. Lancaster, D. L. Hughes, P. N. Horton and M. Bochmann, *Dalton Trans.*, 2006, 2415-2426.
- 64 S. J. Lancaster, A. Rodriguez, A. Lara-Sanchez, M. D. Hannant, D. A. Walker, D. H. Hughes and M. Bochmann, *Organometallics*, 2002, **21**, 451-453.
- 65 M. Bochmann, *Organometallics*, 2010, **29**, 4711-4740.
- 66 M. Gonsior, I. Krossing, L. Müller, I. Raabe, M. Jansen and L. van Wüllen, *Chem. Eur. J.*, 2002, **8**, 4475-4492.
- 67 V. C. Williams, G. J. Irvine, W. E. Piers, Z. Li, S. Collins, W. Clegg, M. R. J. Elsegood and T. B. Marder, *Organometallics*, 2000, **19**, 1619-1621.
- 68 J. Chai, S. P. Lewis, S. Collins, T. J. J. Sciarone, L. D. Henderson, P. A. Chase, G. J. Irvine, W. E. Piers, M. R. J. Elsegood and W. Clegg, *Organometallics*, 2007, **26**, 5667-5679.
- 69 R. E. LaPointe, G. R. Roof, K. A. Abboud and J. Klosin, *J. Am. Chem. Soc.*, 2000, **122**, 9560-9561.
- 70 *US Pat.*, 6 627 573 B2, 2003.
- 71 M. Becker, A. Schulz, A. Villinger and K. Voss, *RSC Adv.*, 2011, **1**, 128-134.
- 72 D. Vagedes, G. Erker and R. Fröhlich, *J. Organomet. Chem.*, 2002, **641**, 148-155.
- 73 J. Zhou, S. J. Lancaster, D. A. Walker, S. Beck, M. Thornton-Pett and M. Bochmann, *J. Am. Chem. Soc.*, 2001, **123**, 223-237.
- 74 L. Falivene, R. Credendino, A. Poater, A. Petta, L. Serra, R. Oliva, V. Scarano and L. Cavallo, *Organometallics*, 2016, **35**, 2286-2293.
- 75 C. García-Morales, B. Ranieri, I. Escofet, L. López-Suarez, C. Obradors, A. I. Konovalov and A. M. Echavarren, *J. Am. Chem. Soc.*, 2017, **139**, 13628-13631.
- 76 V. López-Carrillo and A. M. Echavarren, *J. Am. Chem. Soc.*, 2010, **132**, 9292-9294.
- 77 A. Homs, C. Obradors, D. Leboeuf and A. M. Echavarren, *Adv. Synth. Catal.*, 2014, **356**, 221-228.
- 78 M. E. de Orbe and A. M. Echavarren, *Org. Synth.*, 2016, **93**, 115-126.
- 79 A. Zhdanko and M. E. Maier, *Chem. Eur. J.*, 2014, **20**, 1918-1930.
- 80 G. R. Fulmer, A. J. M. Miller, N. H. Sherden, H. E. Gottlieb, A. Nudelman, B. M. Stoltz, J. E. Bercaw and K. I. Goldberg, *Organometallics*, 2010, **29**, 2176-2179.
- 81 M. E. Voss, C. M. Beer, S. A. Mitchell, P. A. Blomgren and P. E. Zhichkin, *Tetrahedron*, 2008, **64**, 645-651.
- 82 C. G. Anklin and P. S. Pregosin, *J. Organomet. Chem.*, 1983, **243**, 101-109.
- 83 P. de Frémont, N. M. Scott, E. D. Stevens and S. P. Nolan, *Organometallics*, 2005, **24**, 2411-2418.
- 84 A. A. Hagedorn, P. W. Erhardt, W. C. Lumma, R. A. Wohl, E. Cantor, Y. L. Chou, W. R. Ingebretsen, J. W. Lampe and D. Pang, *J. Med. Chem.*, 1987, **30**, 1342-1347.
- 85 *US Pat.*, 6 548 494 B1, 2003.